MARINE AND METEORIC DIAGENESIS OF PLEISTOCENE CARBONATES FROM A NEARSHORE SUBMARINE TERRACE, OAHU, HAWAII

C.E. SHERMAN, C.H. FLETCHER, AND K.H. RUBIN

Department of Geology and Geophysics, School of Ocean and Earth Science and Technology, University of Hawai'i at Manoa, 1680 East–West Road, Honolulu, Hawai'i 96822, U.S.A.

ABSTRACT: **The nearshore slope of Oahu consists of a shallowly dipping shelf extending from the shoreline out to the ~ −20 m contour, where there is a sharp break in slope down to ~ −30 m. Limestones recovered in a series of short cores taken from this nearshore terrace are typical of shallow-marine reef environments and comprise either a branching-coral or massive-coral facies. The composition as well as shoreward zonation of facies suggests that the terrace represents an *in situ* fossil reef complex. Th–U ages of *in situ* corals are all Pleistocene and suggest that the bulk of the feature formed during marine oxygen isotope stage 7. Later accretion along the seaward front of the terrace occurred during marine oxygen isotope substages 5a and/or 5c. Deposition during these interglacial highstands has not previously been documented in the sea-level record on Oahu.**

Although the diagenetic record in the cored samples is incomplete, three periods of diagenesis are identified: early shallow marine, meteoric, and post-meteoric shallow marine. Early shallow-marine diagenesis includes cementation by aragonite and Mg calcite in an active marine phreatic zone and predominantly micritization in a stagnant marine phreatic zone. Meteoric processes occurred in the vadose zone and include precipitation of calcite (needle fibers, meniscus cements, micritic networks), neomorphism, and dissolution. All limestones are now in an active marine phreatic zone. Evidence of post-meteoric shallow-marine diagenesis is found in last-generation Mg calcite cements and internal sediments occurring directly on limestone substrates that have otherwise been stabilized to calcite. The present seafloor is undergoing extensive biological and physical erosion. No Holocene limestones were recovered. Petrographic and geochemical signatures of subaerial exposure and meteoric diagenesis are recognized within the upper several centimeters of all cores. Thus, the present seafloor in the study area is a flooded Pleistocene subaerial exposure surface.

INTRODUCTION

The island of Oahu (Fig. 1) has been important in late Quaternary sea-level studies (e.g., Veeh 1966; Ku et al. 1974). Oahu contains an extensive and complex sedimentary carbonate record in the form of emerged and submerged shorelines (preserved intertidal notches) and shelves (coral and coralline algal reef complexes) (cf. Stearns 1946, 1978). Following the work of Stearns, investigations of carbonates on Oahu have focused, almost exclusively, on radiometric dating of emerged marine deposits in order to establish and constrain the timing of Quaternary interglacial sea levels (e.g., Veeh 1966; Ku et al. 1974; Muhs and Szabo 1994; Szabo et al. 1994; Fletcher and Jones 1996; Grossman and Fletcher 1998). Sedimentologic and petrologic data are an integral component of paleoenvironmental studies, and thus paleo-sea-level interpretations. However, there have been few sedimentary petrologic studies of uplifted carbonates in Hawaii (e.g., Meyers 1987; Sherman et al. 1993). In addition, the nearshore submarine record has received very limited study.

The work of Stearns (1974, 1978), Coulbourn et al. (1974), and Fletcher and Sherman (1995) clearly identified morphological features on the submarine slopes of Oahu formed by relative sea levels lower than present. The shallow submarine slope of Oahu is characterized by a stepped topography consisting of broad terraces separated by eroded, vertical scarps bearing intertidal notches and other erosional features typically associated with former shorelines. An understanding of the mode and timing of their formation is absent from our knowledge of the Quaternary history of Oahu. During the late Quaternary, eustatic sea level has fluctuated between ~ 6 m above and ~ 130 m below present sea level (Chappell and Shackleton 1986; Shackleton 1987). Presumably, these sea-level fluctuations were accompanied by vertical migration of marine and meteoric environments within the nearshore sediments of Oahu. Both of these diagenetic environments can leave characteristic petrographic and geochemical features.

In this paper, we describe depositional facies and report radiometric data that indicate the mode and timing of formation of the nearshore terrace. We also present petrographic and geochemical evidence of early shallow-marine, meteoric, and post-meteoric shallow-marine diagenesis. In addition, we discuss the extent to which the sedimentary petrology of these deposits augments our present understanding of near-shore Quaternary environments on Oahu.

GEOLOGIC SETTING

Oahu (21°27′ N, 158° W) is a high volcanic island within the 3500 km long Hawaii–Emperor island–seamount chain. It is composed primarily of the eroded remnants of two great shield volcanoes. Pleistocene sedimentary carbonates, deposited in subtidal reef to supratidal dune environments, also form an important aspect of the geology of the island and are more extensive on Oahu than on any other of the main Hawaiian islands.

Oahu has, in the past, been characterized as a "stable tectonic setting" and suitable for use as a global datum for Quaternary sea levels (e.g., Veeh 1966; Ku et al. 1974; Stearns 1978; Moore 1987). However, geophysical investigations (Watts and ten Brink 1989) and analyses of Pleistocene limestones on Oahu (Jones 1993, 1994; Muhs and Szabo 1994; Szabo et al. 1994) indicate that the island has been undergoing gradual uplift during the late Quaternary attributed to lithospheric flexure associated with volcanic loading at the Big Island of Hawaii. Elevations and ages of emergent Pleistocene limestones on Oahu indicate that Oahu has experienced nearly 30 m of uplift since ~ 500 ka at an average rate of 0.05 to 0.06 m per 1000 years.

Our study area lies on the leeward side of Oahu between Maili and Kepuhi Points. Nearshore topography consists of a shallowly dipping shelf extending from the shoreline out to the ~ −20 m contour, where there is a sharp break in slope down to ~ −30 m, where a deeper terrace begins. The width of this shelf varies from ~ 0.5 km at Kepuhi Point to ~ 1.8 km at Maili and Waianae. The seafloor consists of lithified limestone with a thin veneer of loose carbonate sand and sparse, patchy occurrences of coral and coralline algal growth. In some areas, a prominent notch is carved into the seaward front of the nearshore terrace at ~ −24 m (Fig. 2). Stearns (1974) named this feature the Kaneohe Shoreline and proposed that it was formed in the late Pleistocene at ~ 80 ka. For purposes of discussion, the nearshore terrace is divided into three zones based on depth and relationship to the present morphology of the terrace (Fig. 3). These zones are: zone 1, the inner part of the terrace, < 10 m water depth; zone 2, proximal to the seaward margin of the terrace, 10–20 m water depth; zone 3, seaward of the slope break, 20–35 m water depth.

METHODS AND NOMENCLATURE

Cores were collected via a diver-operated Tech 2000 submersible, hydraulic, rotary coring drill with a 7.6 cm diameter diamond-studded drill

JOURNAL OF SEDIMENTARY RESEARCH, VOL. 69, NO. 5, SEPTEMBER, 1999, P. 1083–1097
 1073-130X/99/069-1083/$03.00

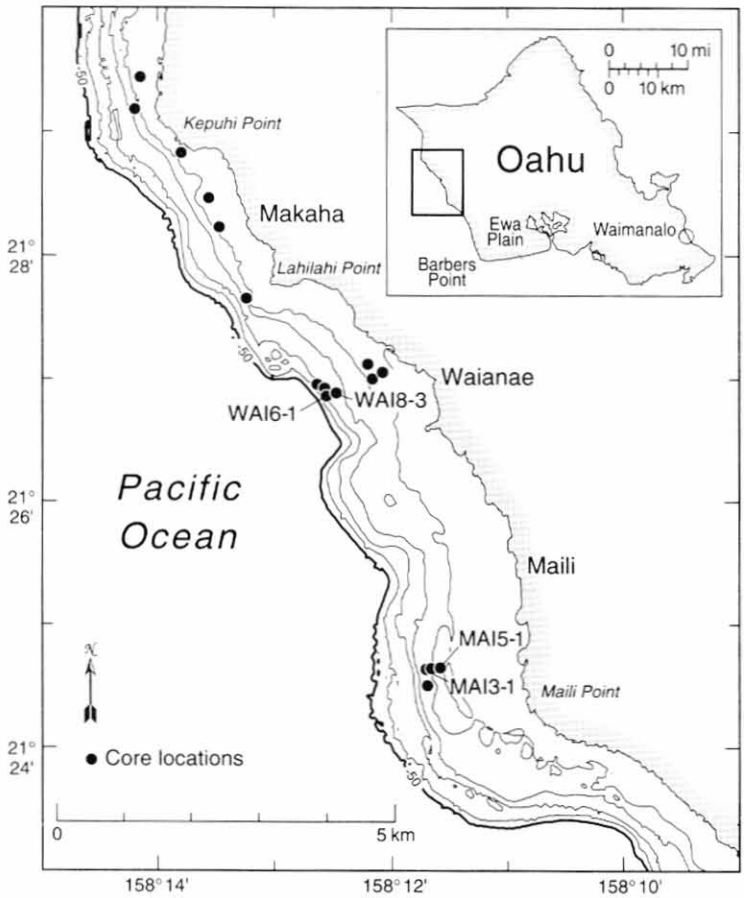

FIG. 1.—Location map showing core sites along leeward Oahu.

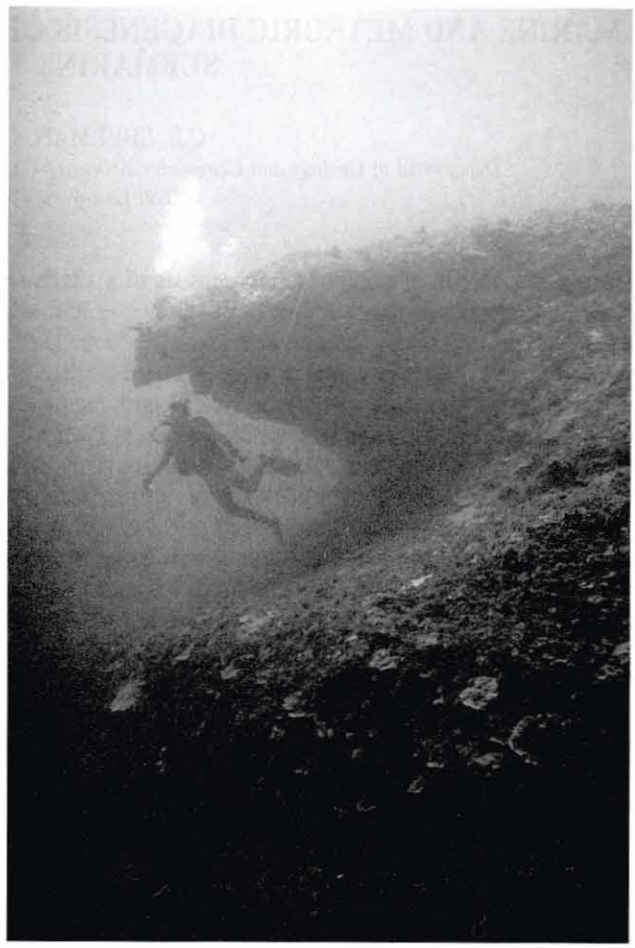

FIG. 2.—The −24 m Kaneohe Shoreline carved into the seaward front of the shallow terrace.

bit. All cores were collected between ~ 5 and 35 m water depth along ~ 10 km of shoreline on the leeward coast of Oahu. Recovered cores averaged ~ 62 cm in length, with a maximum of 205 cm. The percentage of recovery averaged ~ 90%. Limestones were classified according to Dunham's (1962) scheme as modified by Embry and Klovan (1971).

The cores were sampled for radiometric, petrographic, mineralogic, and geochemical analyses, taking care that each lithofacies as well as obvious diagenetic features within a core were sampled. Approximately 50 thin sections were analyzed petrographically. Terminology for describing microfabrics follows the recommendations of Rezak and Lavoie (1993). Duplicates were made of a portion of the thin sections for staining for Mg calcite following the method of Choquette and Trusell (1978).

Carbonate mineralogy was determined with a Scintag Pad V powder X-ray diffractometer (XRD) with a solid state Ge detector using Cu Kα radiation. Calcite-to-aragonite composition ratios were determined using a standard curve generated from the peak area ratios (111 aragonite peak, 104 calcite peak) of known mixtures of aragonite and calcite (Sabine 1992). The mole percentages of $MgCO_3$ of magnesian calcite phases were determined from the offset of the *d* spacing of the 104 Mg calcite peak from the *d* spacing of the 104 peak of pure calcite (Bischoff et al. 1983). The term magnesian calcite or Mg calcite refers to those metastable calcites with greater than 5 mole % $MgCO_3$. Calcite with less than 5 mole % $MgCO_3$ is simply referred to as calcite (cf. Scoffin 1987). All mineralogic data represent the average of two duplicate analyses.

Major and minor elements (Ca, Mg, Sr, Fe, Mn) in components and cements were quantitatively measured with a Cameca SX50 electron microprobe. Parameter settings were: 5 μm beam diameter, 15 kV accelerator voltage, and 15 nA beam current, counting times 60 s (peak and background) for Mg, Sr, Fe, and Mn, 30 s (peak) and 15 s (background) for Ca. In all cases Mn was below detection limits and, therefore, is not reported here. With the exception of some microcrystalline cements, Fe was also below detection limits. Mg and Sr are used as key indicators of mineralogy of cements in this study. The relative errors are 1% for Mg at a measured value of 17 mole % $MgCO_3$, 4% for Sr at a measured value of 7000 μg/g, and 8% for Fe at a measured value of 5000 μg/g.

The absolute age of fossil corals was determined using the ^{230}Th–^{234}U–^{238}U technique. Sample chips were ultrasonically cleaned in ultra-pure reagents and powdered. Only those samples with < 3% calcite (determined by XRD) were dissolved for Th and U isotopic analysis and spiked with ^{229}Th and ^{233}U. Techniques for Th and U isotopic analysis of corals in the SOEST Isotope Lab are modified after those of Edwards et al. (1986/87). Total procedural blanks for this chemistry were 1–5 pg U and 5–10 pg Th. Analyses were conducted in single-collector ion-counting mode by peak-jumping on a VG Sector 54 mass spectrometer outfitted with a WARP abundance sensitivity filter after the magnetic sector and an ion-counting Daly. Linearity of the ion counter is within counting statistics everywhere within the range 10 cpm to 2×10^6 cpm (as determined by analysis of external standards). All ion-counting data is corrected for a Daly Bias of 0.58 ‰/amu relative. Fractionation of U isotopes was calibrated by analysis of external standards (natural U and U010). External reproducibility of $^{234}U/^{235}U$ is 0.25% prior to fractionation correction and < 0.10% after correction. Precision of fractionation corrected $^{234}U/^{235}U$ is ~ 0.10% (standard deviation of 10 measurements).

FACIES

Massive-Coral Facies

The massive-coral facies (Fig. 4) consists of *in situ* coral and coralline–algal framework along with coarse skeletal grainstones and rudstones that

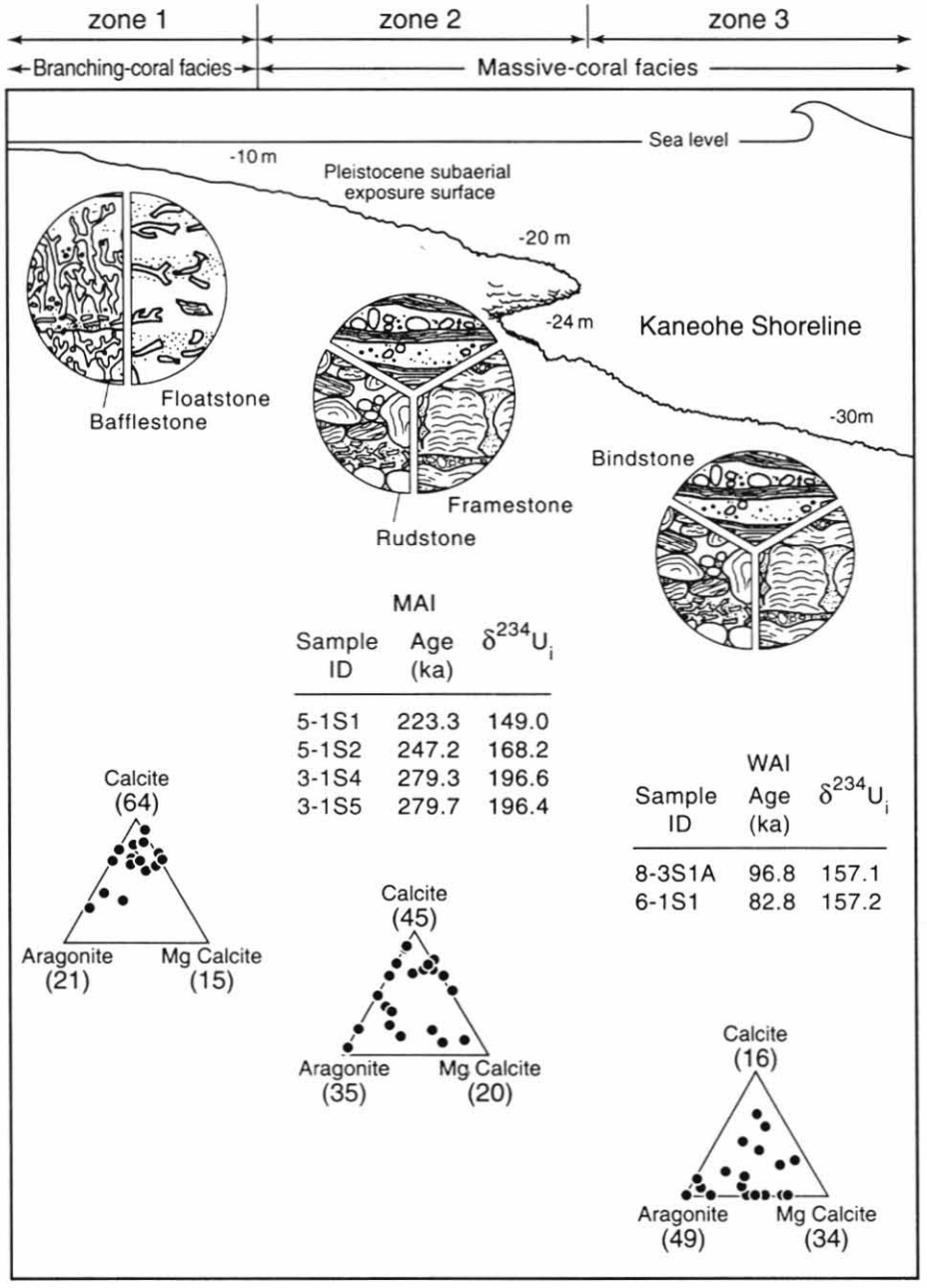

FIG. 3.—Schematic profile of nearshore terrace showing relative locations of zones 1, 2, and 3. **TOP)** Zonation of lithofacies along terrace profile: zone 1, < -10 m, is composed primarily of bafflestones and floatstones that constitute the branching-coral facies; zone 2, -10 to -20 m, and zone 3, -20 to -35 m, are composed of coral-algal framestones and bindstones and skeletal rudstones that constitute the massive-coral facies. Relative location of the -24 m Kaneohe Shoreline is also shown. **MIDDLE)** Th–U ages and initial $\delta^{234}U$ ($\delta^{234}U_i$) values of *in situ* fossil corals. MAI samples are from zone 2. WAI samples are from zone 3. **BOTTOM)** Bulk mineralogy of samples from zones 1, 2, and 3. Dots indicate mineralogy of individual samples. Numbers in parentheses indicate the average composition of samples (in weight percent) within each zone.

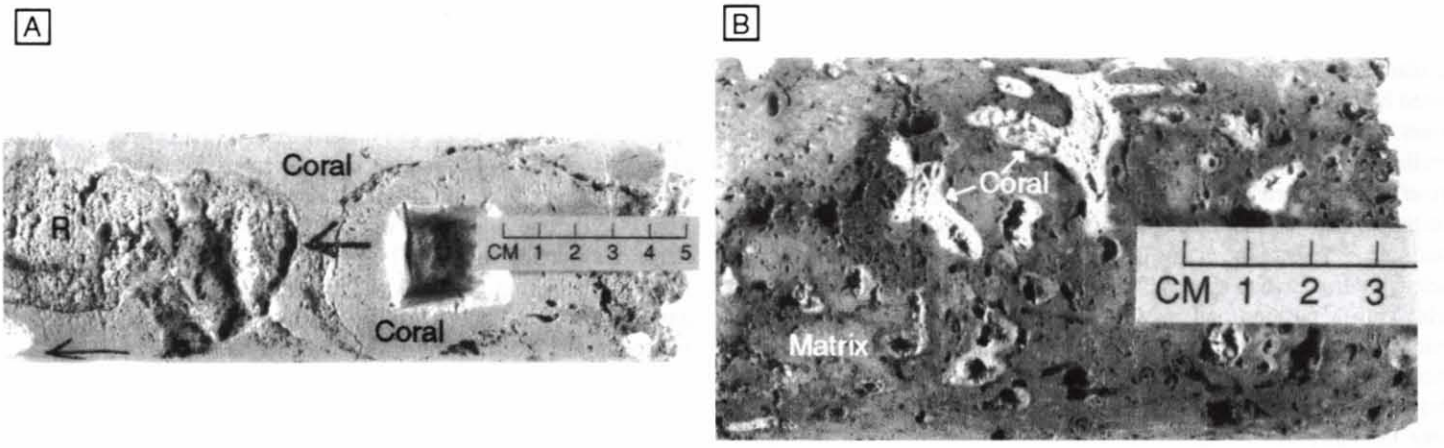

FIG. 4.—Pleistocene lithofacies found in the nearshore terrace. **A)** Massive-coral facies composed of *in situ* framework of massive corals (*Porites lobata*) and a skeletal rudstone (R) filling framework voids. **B)** Branching-coral facies composed of delicate branching corals (*Pocillopora damicornis*) in a lime-mud matrix.

TABLE 1.—*Uranium and thorium isotopic composition and ^{230}Th ages of submerged Oahu corals.*[1]

Sample	Depth (m)	U (ng/g)	Th (pg/g)	$^{232}Th/^{238}U$ (atomic ratio)	$[^{230}Th/^{238}U]$ activity	Age (ka)	$\sigma^{234}U$ measured[2]	$\sigma^{234}U$ initial[2]
MAI5-1S1	10	2779 ± 7	60.0 ± 2	$2.232 \pm 8 \times 10^{-5}$	0.9584 ± 48	223.3 ± 1.4	79.1 ± 1	149.0 ± 1.0
MAI5-1S2	10	2719 ± 7	556.0 ± 9	$2.113 \pm 6 \times 10^{-4}$	0.9926 ± 48	247.2 ± 1.5	83.5 ± 1	168.2 ± 1.1
MAI3-1S4	13	2656 ± 6	75.1 ± 2	$2.920 \pm 9 \times 10^{-5}$	1.0303 ± 51	279.3 ± 1.8	89.0 ± 1	196.6 ± 1.3
MAI3-1S5	13	2709 ± 7	99.4 ± 2	$3.790 \pm 12 \times 10^{-5}$	1.0304 ± 50	279.7 ± 1.8	88.9 ± 1	196.4 ± 1.2
WAI8-3S1A	27	2709 ± 7	47.5 ± 1	$1.814 \pm 7 \times 10^{-5}$	0.6688 ± 33	96.8 ± 6	119.4 ± 1	157.1 ± 1.0
WAI6-1S1	30	3085 ± 8	227.0 ± 4	$7.604 \pm 24 \times 10^{-5}$	0.6068 ± 30	82.8 ± 5	124.3 ± 1	157.2 ± 1.0

[1] Activities are calculated using the following: $\lambda_{230} = 9.195 \times 10^{-6}$ yr^{-1} (Meadows et al. 1980). $\lambda_{234} = 2.835 \times 10^{-6}$ yr^{-1} (Lounsbury and Durham 1971; de Bievre et al. 1971). $\lambda_{238} = 1.551 \times 10^{-10}$ yr^{-1} (Jaffrey et al. 1971). Analyses conducted on 0.2 to 0.3 g of material. Data is corrected for procedural blanks (<6 pg each for Th and U). Reported errors include both 1σ analytical error and errors in λ values.
[2] $\delta^{234}U = [^{234}U/^{238}U$ activity ratio $- 1] \times 1000$.

may fill voids in the framework as well as constitute entire core sections. The predominant corals are massive colonies of *Porites lobata,* a coral that in Hawaii is most common on wave-exposed reef slopes between depths of 3 and 15 m (Maragos 1977). Crustose coralline algae are also an important component of the massive-coral facies, where they occur as sheet-like encrustations on the upper surfaces of corals, lining voids in the coral framework, over previously lithified rudstone, as well as coating larger coral clasts in the rudstones. The encrusting foraminifer *Homotrema* is also common. Vermetid gastropods and serpulid worms are present but rare. Associated skeletal grainstones and rudstones are composed predominantly of fragments of the framework-forming corals and coralline algae, as well as reef-associated organisms, such as mollusks, echinoderms, and benthic foraminifers. Grains typically range from medium sand through coarse pebbles and are subangular to subrounded, exhibiting poor to moderate sorting. Large clasts are generally encrusted by coralline algae. Mud is also present, but is restricted to protected voids in the framework. The dominance of massive corals (*P. lobata*) and encrusting algae indicates a shallow, high-energy environment of deposition (cf. James 1983; Tucker and Wright 1990; James and Bourque 1992). The combination of a grainstone and rudstone matrix with *in situ* framework is also common in high-energy settings (cf. Bosence 1985). The massive-coral facies is found in zones 2 and 3, i.e., along the seaward margin of the terrace. This distribution is consistent with expected zonation of lithofacies in a marginal reef complex, where rudstones and framestones are most common in reef flat, reef crest, and reef front environments (cf. James and Bourque 1992).

Branching-Coral Facies

The branching-coral facies is composed of delicate branching corals, coralline algae, and associated biota set in a lime-mud matrix forming *in situ* bafflestones, floatstones, or wackestones. It is differentiated from the massive-coral facies by its mud-supported fabric and the presence of delicate branching corals, such as *Pocillopora damicornis.* In Hawaii, this coral is usually found in protected bays or upon the inner parts of large reef flats away from breaking waves (Maragos 1977). The floatstones and wackestones are generally poorly sorted and contain silt- to pebble-size, angular skeletal clasts, as well as subangular to subrounded peloids, supported by a lime-mud matrix. Grains constitute ~ 10–20% of these limestones. Skeletal grains are predominantly fragments of branching corals and coralline algae, but also include mollusks, foraminifers, and echinoderms. Preservation of skeletal components varies from poor to good. Boring, micritization, and micrite envelopes are common. Sand-size peloids, which constitute ~ 20% of the grains in this facies, probably represent micritized skeletal grains. Branching corals and coralline algae are also found in upright, growth position and may have acted as "baffles" trapping fine-grained sediment and forming *in situ* bafflestones. The presence of delicate-branching corals and dominance of lime-mud matrix indicate a low-energy environment of deposition. The branching-coral facies is found in zone 1, along the inner part of the terrace landward of the massive-coral facies. The distribution of the branching-coral facies is consistent with the expected zonation of lithofacies in a marginal reef complex, where bafflestones and floatstones are most common in back-reef environments (cf. James and Bourque 1992).

TH–U AGES OF PLEISTOCENE CORALS

Absolute ^{230}Th–^{234}U–^{238}U ages of six nearly pristine (> 97% aragonite) corals of the species *Porites lobata* were determined from high-precision TIMS isotopic composition determinations at the University of Hawaii (Table 1, Fig. 3). These samples came from four different cores (two each from cores MAI3–1 and MAI5–1 and one each from cores WAI6–1 and WAI8–3). Calculated ages fall into three groupings, which correspond to the cores from which they were sampled: corals from cores MAI3–1 and MAI5–1 have ages of 279.1 to 279.6 ka and 223.1 to 247.0 ka, respectively; corals from the more seaward cores WAI6–1 and WAI8–3 have ages of 82.8 and 96.8 ka, respectively. These sample ages confirm a Pleistocene age for this nearshore terrace/reef complex. Importantly, no Holocene samples were recovered at any of the four sites.

Before interpreting these ages further, it is necessary to assess their relative quality and reliability. All dated corals were > 97% aragonite, which indicates that replacement by calcite has played a minimal role. Our dated corals contain between 2719 ng/g and 3085 ng/g U (Table 1), which is well within the range of other Hawaiian corals (e.g., 2310 to 3460 ng/g for > 30 Pleistocene corals; Szabo et al. 1994) indicating that wholesale addition or loss of U, if it has occurred, has been minimal. Th/U ratios are more variable in our data set (Table 1), ranging from 1.8×10^{-5} to 2.1×10^{-4}. However, even the highest Th/U value in our sample set is well within the range of Th/U found in otherwise pristine corals from various localities worldwide.

The most stringent test of age reliability arises from a comparison of the ^{230}Th-age-corrected $^{234}U/^{238}U$ (or $^{234}U/^{238}U_i$) with that of modern seawater (activity ratios in modern sea water range from 1.146 to 1.150, or 146 to 150‰ using the $\delta^{234}U$ convention; Chen et al. 1986). Modern and Holocene-age corals have $\delta^{234}U_i$ of 145 to 155‰ (Bard et al. 1996a; Bard et al. 1996b, and references therein). On the basis of these results, $\delta^{234}U_i$ has been accepted as a "working definition" of ^{230}Th–^{234}U–^{238}U age quality, with samples having $\delta^{234}U_i$ ranging from 145 to ~ 150‰ being considered highly reliable, those with $\delta^{234}U_i$ ranging from 150 to 160 or 165‰ being moderately reliable, and those in excess of 165‰ being significantly less reliable (e.g., Szabo et al. 1994; Bard et al. 1996b). Although only three of the six corals in the present data set rigorously conform to the "acceptable category" as just defined (samples WAI6–1S1, WAI8–3S1A, and MAI5–1S1), one additional sample (MAI5–1S2) is barely outside this range, considering its stage 7 age (Fig. 5). The other two (pre–stage 7) samples, both from core MAI3–1, have clearly compromised $\delta^{234}U_i$, on any measurement scale. Both of these samples contained < 3% calcite, indicating that replacement of original coral aragonite by calcite has been negligible. Therefore, possible addition of more recent submarine aragonitic cements may explain the elevated $\delta^{234}U_i$ values.

Using the four most reliable ages of the present data set, the following chronological history can be reconstructed: The upper part of the terrace (zone 2) is constructed of materials aged 223.1 ka (highly reliable) to 247.0

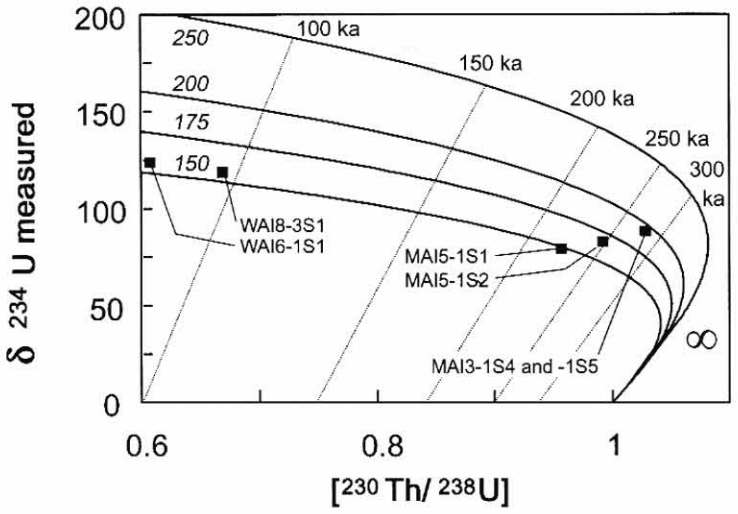

FIG. 5.—Plot of measured $\delta^{234}U$ versus $^{230}Th/^{238}U$ activity ratio of submerged Oahu corals. Correlated *x*-axis and *y*-axis errors on each datum are smaller than the symbol plotted. The solid curved lines are contours of initial $\delta^{234}U$ values ($\delta^{234}U_i$), and dotted lines are contours of ^{230}Th age. The contour for $\delta^{234}U_i = 150‰$ corresponds to the modern marine value. Data that plot along this contour are considered most reliable (see text). Deviation from this contour indicates open-system behavior and, therefore, less reliable ^{230}Th ages.

ka (less reliable), corresponding to the age of marine oxygen isotope stage 7 (Bassinot et al. 1994). In contrast, samples collected at the seaward base of the terrace (zone 3) are significantly younger. Sample WAI8–2S1A, collected at ~ 27 m water depth, has an age of 96.8 ka, which corresponds to marine oxygen isotope substage 5c (97 ka, event 5.3 of Bassinot et al. 1994). ^{230}Th ages of Barbados corals suggests an age of 100.5 ka for marine oxygen isotope substage 5c (Gallup et al. 1994). Sample WAI6–1S1, collected at ~ 30 m water depth, has an age of 82.8 ka, which likely corresponds to marine oxygen isotope substage 5a (79 ka; event 5.1 of Bassinot et al. 1994). The age of sample WAI6–1S1 is also very similar to the ^{230}Th age of a substage 5a coral from Barbados (83.3 ka; Gallup et al. 1994).

MINERALOGIC COMPOSITION OF PLEISTOCENE CARBONATES

The submerged Pleistocene carbonates of Oahu have a variable composition of aragonite, Mg calcite, and calcite (Fig. 3). A few samples contained trace amounts of dolomite, but it is relatively unimportant compared to the other carbonate minerals. Although the average bulk mineralogic compositions of limestones in all three zones include calcite, aragonite, and Mg calcite, there is a general trend of decreasing calcite content from zone 1 to zone 3. Zone 1 limestones have a relatively uniform composition of predominantly calcite (> 60%). Limestones in zone 2 have the broadest range of compositions from uniformly calcite to a mixture of mainly aragonite and Mg calcite. Limestones in zone 3 display a more uniform composition predominantly of aragonite and Mg calcite.

DIAGENETIC PROCESS AND PRODUCTS

Early Shallow-Marine Diagenesis

Evidence of early shallow-marine diagenesis is found in first-generation shallow-marine aragonite and Mg calcite cements (Fig. 6). Aragonite is found exclusively as acicular aggregates, whereas Mg calcite is found in a variety of forms, including microcrystalline, peloidal, and bladed spar. All are common shallow-marine reef cements (Macintyre 1977; Macintyre and Marshall 1988) Acicular aragonite cement is relatively common in the massive-coral facies of zones 2 and 3, but is found exclusively as an intraskeletal syntaxial cement mainly in coral and less frequently in mollusk fragments. Acicular aragonite is absent from the branching-coral facies of zone 1. Overall, it is not an important agent of lithification in the submerged Pleistocene limestones of Oahu. These acicular aragonite cements have an average strontium concentration of 7891 μg/g. $MgCO_3$ content is consistently low, averaging 0.4 mole % $MgCO_3$. The high strontium and low magnesium concentrations found in the acicular aragonite cements are typical of aragonite cements precipitated from normal seawater (Macintyre 1977; Macintyre and Marshall 1988). When multiple generations of cement are present in intraskeletal pores in coral skeletons, syntaxial acicular aragonite is the first cement, a common relationship that has been reported at several locales (cf. Ginsburg et al. 1971; James et al. 1976). Macintyre (1977) and Lighty (1985) observed that syntaxial acicular aragonite forms just below the living tissue and surface of active skeletal accretion in corals. They concluded that its formation is probably contemporaneous with coral growth. Thus, the presence of syntaxial acicular aragonite in the massive-coral facies provides good evidence of early marine diagenesis contemporaneous with deposition. In addition, syntaxial acicular aragonite cements are in some cases engulfed in secondary, void-filling calcite spar cement, which indicates their formation prior to the onset of meteoric diagenesis (see Fig. 6).

Microcrystalline Mg calcite is the most common type of cement found in the submerged Pleistocene limestones of Oahu and is most prevalent in the massive-coral facies in zones 2 and 3. It forms coatings and crusts ~ 10–60 μm thick on grains and the walls of intraskeletal and framework cavities, and as the matrix of internal sediment. The microcrystalline coatings are commonly overgrown by a 5–10 μm thick fringe of clear, bladed microspar. While microcrystalline Mg calcite generally forms the first generation of cement, it also forms coatings on previous generations of cement, such as acicular aragonite, bladed spar, and equant spar. Sharp boundaries separate cement from substrates. This, along with its distribution as linings on the walls of intragranular and intraskeletal pores, is a good indication that the microcrystalline coatings are a cement rather than a product of boring organisms. Peloids formed of Mg calcite are also common, being found mainly in protected intragranular, intraskeletal, and framework pores where peloids are protected from compaction and commonly form geopetal structures. Well-defined peloids (~ 20–60 μm in diameter) have a clear, dentate rim of microspar that tends to reduce interpeloidal porosity (cf. Lighty 1985; Macintyre 1985). Bladed Mg calcite microspar is commonly present on cavity walls that contain peloidal Mg calcite.

Microcrystalline Mg calcite also forms lithified micritic crusts (Macintyre 1977; Marshall 1983; Macintyre and Marshall 1988) in the massive-coral facies of zones 2 and 3. The crusts are lithified deposits of microcrystalline, commonly peloidal, Mg calcite with varying amounts of internal sediment that form coatings ~ 0.1 to 5.0 cm thick on the upper surfaces of corals and associated encrusting organisms (coralline algae, foraminifera, vermetids, serpulids, etc.), in cavities in the reef framework, and over previously lithified grainstones and rudstones. The crusts generally fill intraskeletal cavities and borings at the outer edges of the corals that they coat. The crusts are found in laminated and columnar forms (Fig. 6). Laminated crusts generally have a smooth surface, display wavy, often discontinuous laminae ~ 0.5 to 1.0 mm thick, and may have a domal shape. Columnar crusts have an irregular, "knobby" surface, which is the expression of club-shaped protuberances ~ 3 to 30 mm high. The knobs may be a result of the differential accretion of microcrystalline or peloidal Mg calcite or in some cases the presence of buried encrusting organisms (e.g., Macintyre 1977, 1984; Marshall 1983). In some instances columnar crusts may form on top of laminated crusts. In modern environments, micritic crusts develop within reef structures, generally in areas close to the reef surface and where marine cementation is particularly active (Macintyre and Marshall 1988; Scoffin 1993). The micritic crusts found in the Oahu cores contain an average of 15.0 mole % $MgCO_3$ and 1321 μg/g strontium.

Along with micrite and peloids, bladed microspar and spar is a common cement in the submerged limestones of Oahu. It is found as isopachous

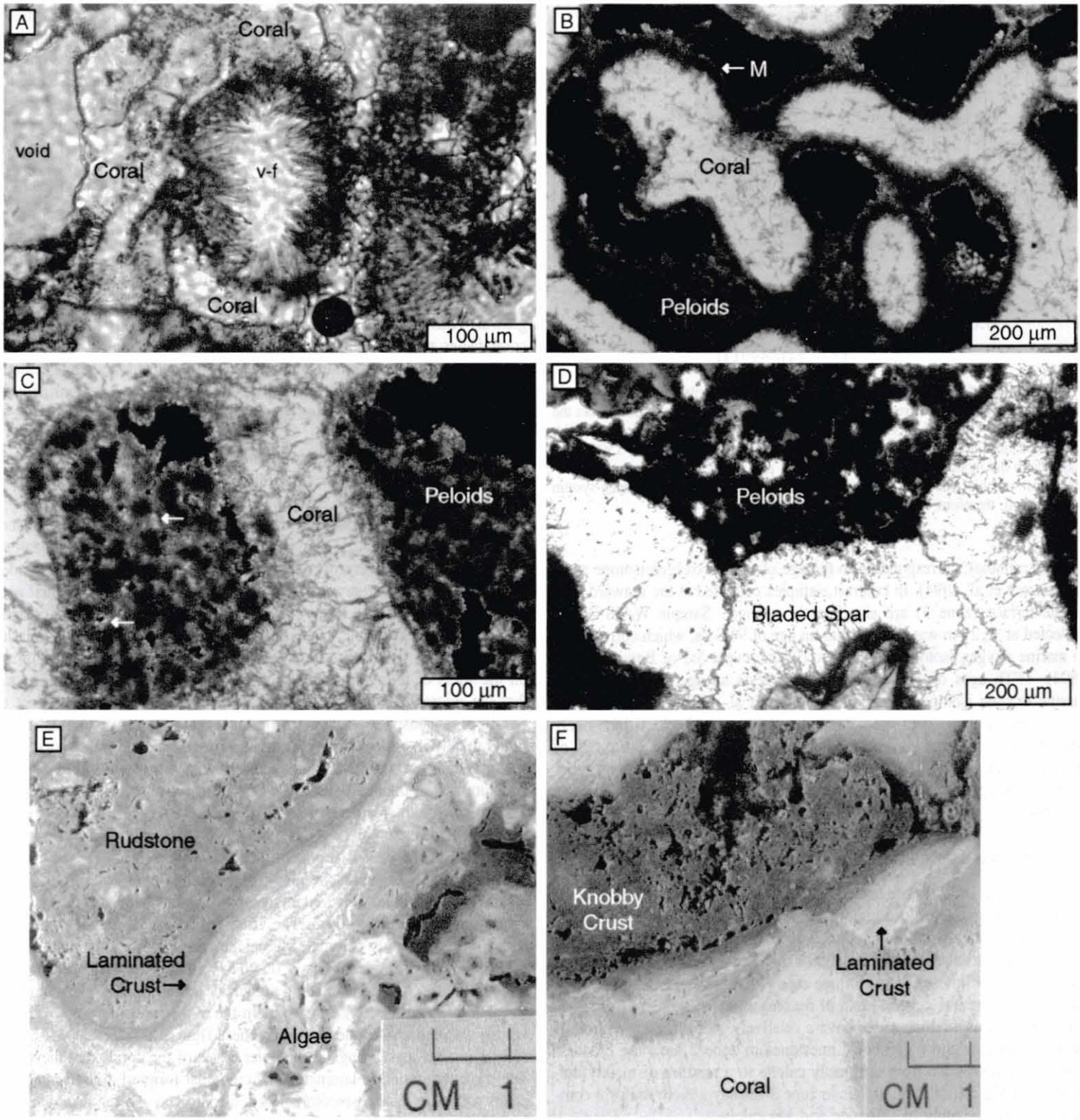

FIG. 6.—Submarine cements. **A)** Original marine syntaxial acicular aragonite cement lining intraskeletal cavities in coral and engulfed distally by secondary void-filling calcite spar cement (v-f). Coral altered to neomorphic spar. Thin section, plane-polarized light. **B)** Coral with coating of microcrystalline Mg calcite cement and peloidal Mg calcite cement partially filling intraskeletal cavities forming geopetal structure. Thin section, crossed polars. **C)** Close-up of peloidal Mg calcite showing clear, dentate rim of Mg calcite microspar (arrows) reducing interpeloidal porosity. Thin section, crossed polars. **D)** Void lined by isopachous rim of bladed Mg calcite spar. Bladed spar overlain by peloidal Mg calcite. Thin section, plane-polarized light. **E)** Laminated micritic crust (extending diagonally from upper right to lower left) over crustose coralline algae in massive-coral facies. Lithified skeletal rudstone occurs over micritic crust. **F)** Laminated micritic crust overlain by knobby micritic crust on coral skeleton in massive-coral facies. Note that dark microcrystalline Mg calcite fills outer edge of coral skeleton.

rims coating and sometimes binding grains, but more frequently lining the walls of reef cavities and intraskeletal pores, mainly corals. Individual crystals are ~ 5–100+ µm long. They generally show a gradual increase in width along their length and then have an obtuse pyramid termination. The distribution of microspar versus spar is largely a function of grain and pore size, with larger crystals lining the larger pores. Bladed Mg calcite is commonly found in close association with microcrystalline Mg calcite and may have an inner zone of microcrystalline to peloidal Mg calcite. A similar relationship has been described by James et al. (1976) and Marshall (1983). Bladed Mg calcite cement may be produced by continued growth on the

upper faces of rhombs constituting microcrystalline Mg calcite cement (Longman 1980; Pierson and Shinn 1985).

In the zone 3 massive-coral facies, first-generation Mg calcite cements have largely retained their original composition. The microcrystalline cements contain an average of 13.3 mole % $MgCO_3$ and 802 μg/g strontium. The peloidal carbonate contains an average of 14.4 mole % $MgCO_3$ and 916 μg/g strontium. The bladed cements contain an average of 15.8 mole % $MgCO_3$ and 994 μg/g strontium. These values are consistent with the expected composition of marine Mg calcite cements (cf. Macintyre 1977; Macintyre and Marshall 1988). In addition, the similarity of magnesium and strontium contents among the microcrystalline and sparry cements examined here lends additional support to a precipitate origin for the microcrystalline and peloidal Mg calcite.

The first-generation microcrystalline, peloidal and bladed cements in the zone 2 massive-coral facies have a more variable as well as lower mean $MgCO_3$ content as indicated by both staining and microprobe analyses. Some have retained their original high $MgCO_3$ content, consistent with formation in the marine environment. Others have a low to intermediate $MgCO_3$ content. Variation and lower mean concentration of magnesium is common in marine Mg calcite cements that have been exposed to meteoric diagenesis (cf. Videtich 1985; Vollbrecht and Meischner 1996). Thus, first-generation Mg calcite cements with variable $MgCO_3$ contents probably formed prior to meteoric alteration. Additional evidence of early shallow-marine cementation is found in the fabric and trace-element geochemistry of neomorphic spar. In some instances, large neomorphic crystals replacing coral aragonite display a unique zonation with respect to magnesium and strontium (Fig. 7). Microprobe analyses show that the part of the crystal that was formerly aragonitic coral (identified by its darker color) has an elevated strontium and low magnesium content, properties consistent with calcitization of aragonite (Sandberg 1985). In contrast, parts of the crystal outside the original coral boundary have a relatively low strontium and intermediate magnesium content. This zone of intermediate magnesium content, with an average of 8.3 mole % $MgCO_3$ versus an average of 2.4 mole % $MgCO_3$ in adjacent void-filling equant calcite cements, forms an isopachous rim with a vague sawtooth (bladed) outline around the coral skeleton. It is likely that the coral originally had a lining of bladed Mg calcite spar, a product of early marine cementation, prior to the onset of meteoric diagenesis and neomorphic replacement. The delicate replacement process of calcitization presumably took place via a very thin film such that a single crystal could replace both aragonitic coral and fringing Mg calcite cement, while preserving relic structures as well as the original relative distributions of trace elements. Other calcitized corals have a dark micritic coating that is enriched in magnesium relative to secondary void-filling calcite spar cement and probably represents an early-marine microcrystalline cement (Fig. 8).

In contrast to the massive-coral facies, the branching-coral facies of zone 1 contains very little evidence of early marine cementation. These limestones are supported by a lime-mud matrix. Micritization appears to be the dominant early marine process in the branching-coral facies, where up to 20% of skeletal grains may be micritized. Generally grains are initially bored around the margins and the holes filled with microcrystalline sediment or cement creating a micrite envelope. Micritized grains may also be a result of syndepositional recrystallization of skeletal carbonate to equant micritic fabrics (Reid et al. 1992; Macintyre and Reid 1995, 1998). Micritization of grains takes place in nearly all shallow-marine carbonate settings but is most common in lower-energy settings, where there is little sediment movement. The abundance of micritized grains in the branching-coral facies is consistent with a low-energy environment of deposition.

Subaerial Exposure and Meteoric Diagenesis

During periods of emergence, limestones of the nearshore submarine terrace underwent the meteoric processes of cementation by calcite, neomorphism, and dissolution. Meteoric alteration is patchy on all scales, and there is a range of preservation of original skeletal components from seemingly pristine to completely altered. The zones 1 and 2 limestones display more evidence of meteoric alteration than the younger limestones of zone 3. The zone 2 massive-coral facies displays a broader range of preservation than the adjacent branching-coral facies of zone 1, which is more completely and uniformly altered.

Meteorically derived calcite forms needle fibers, anastomosing micritic networks (alveolar texture), and equant calcite (Fig. 9). Calcite needle fibers (James 1972; McKee and Ward 1983) form random and tangential fabrics occupying intragranular and intergranular voids. Tangential needle fibers are indicative of caliche facies. Random calcite needle fibers are common in caliche profiles and the upper parts of karst profiles and are good indicators of vadose-zone diagenesis. The needle-fiber calcite examined contains an average of 2.3 mole % $MgCO_3$. This value is consistent with precipitation in a meteoric environment. Anastomosing micritic networks and clotted micrite are found in close association with the calcite needle fibers. In some instances the anastomosing networks are actually composed of tangential needle fibers coated by microcrystalline to finely crystalline calcite. The close association of needle fibers, alveolar texture, and clotted micrite is a good indication of subaerial exposure and vadose diagenesis (Esteban and Klappa 1983; Bain and Foos 1993).

In addition to carbonate products, red, iron-rich, noncarbonate clays are incorporated into the limestones and form void and grain coatings (Fig. 9). Reddish-brown discoloration of submarine host sediment is discernible at macroscopic and microscopic scales. The iron-rich clay coatings are an indication of soil formation. The clays may have been carried by colloidal suspension into the limestone (cf. Esteban and Klappa 1983; Bain and Foos 1993).

Equant calcite microspar (5–20 μm) and spar ($>$ 20 μm) are clear, polygonal, equigranular crystals that are found as intergranular and void-fill cements (cf. Whittle et al. 1993). In the terrace limestones of Oahu equant calcite has a patchy distribution. It is most prevalent in samples from zones 1 and 2, the upper/older parts of the terrace, where it is found mainly as a drusy, void-filling cement with crystal sizes ranging from 5 to 150 μm (Fig. 9). Interparticle equant cements are rare and typically form a meniscus texture (Dunham 1971). The equant calcite cements studied contain an average of 2.3 mole % $MgCO_3$ and 1029 μg/g strontium. The distribution, fabric, and composition of these equant cements are consistent with formation in a meteoric vadose setting.

In the cored Pleistocene limestones neomorphism is largely restricted to zones 1 and 2, with over 50% of samples from these zones displaying evidence of neomorphism. Calcitization of aragonitic coral skeletons has resulted in replacement of their original skeletal microstructure by a mosaic of calcite spar (Figs. 7, 8). Although the original spherulitic fascicle fabric is destroyed, the outline of the coral skeletons is clearly discernible as a dark line and residual organic matter imparts a darkened (brownish) appearance to the originally skeletal neomorphic spar (cf. Pingitore 1976; Sandberg 1985). Adjacent pore-filling equant calcite cements are generally clear. The altered corals display fabric-selective mosaics, in which the individual calcite crystals in the original coral skeleton rarely extend beyond the original coral boundaries into void-filling cement (see Fig. 8) and, thus, are controlled by the original skeletal architecture. Pingitore (1976) has shown that corals altered in the vadose zone exhibit fabric-selective calcite mosaics. The replacement mechanism was presumably via a very thin film of fluid.

Mg calcite skeletal grains, such as coralline algae, have largely retained their skeletal microstructure (at the level of petrographic microscope examination). However, staining and microprobe analyses indicate that they have lost Mg^{2+} and are now composed of calcite. Loss of Mg^{2+} may be a result of repetitive intracrystal incongruent dissolution–precipitation in a meteoric environment, as proposed for similarly altered porcelaneous foraminifera by Budd and Hiatt (1993). Aggrading neomorphism of lime-mud

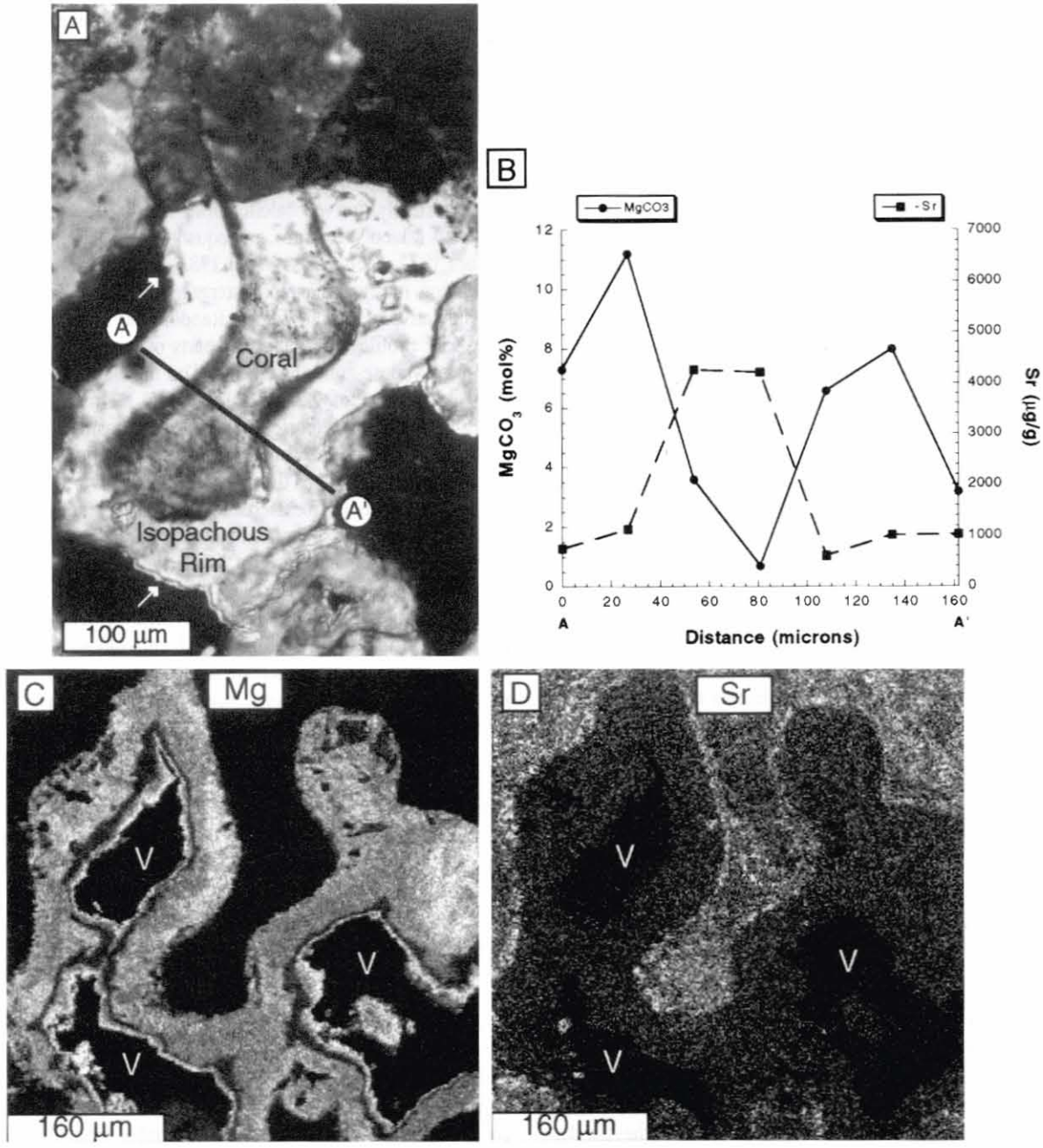

FIG. 7.—Neomorphism of coral and pore-lining, marine Mg calcite cement. **A)** Large crystal of neomorphic spar encompasses both coral skeleton and isopachous rim cement. Residual organic matter imparts a darkened appearance to the former coral skeleton, while the surrounding isopachous rim cement is generally clear. Note the uniform thickness of the rim and sawtooth (bladed) outline of crystal (arrows). Thin section, crossed polars. **B)** Microprobe traverse of $MgCO_3$ (filled circles) and Sr (filled squares) across single crystal of neomorphic spar (A to A'). $MgCO_3$ is elevated in the parts of the crystal outside the original coral boundary. The coral skeleton is enriched in Sr, which is consistent with its original aragonite mineralogy. **C)** Microprobe map of Mg. Density of white spots reflects abundance of Mg. Mg is elevated in parts of the crystals outside the original coral boundary (V = void space). **D)** Microprobe map of Sr. Density of white spots reflects abundance of Sr. Sr is elevated in parts of the crystals within the original coral skeleton (V = void space).

matrix is evident as irregular patches of neomorphic calcite microspar found within the matrix. Neomorphism in the submerged Pleistocene limestones of Oahu is patchy both within and between cores. The patchy distribution of neomorphic fabrics along with the fabric-selective calcite mosaics in altered corals is consistent with neomorphism occurring in the meteoric vadose zone.

Dissolution is most evident in limestones from zones 1 and 2 and is visible on both macroscopic and microscopic scales (Fig. 10). Aragonitic mollusk and coral grains are preferentially dissolved, leaving behind moldic pores. On a macroscopic scale these external molds retain an impression of the surface form of the dissolved coral or mollusk. In some cases a mollusk shell has been filled by lime mud that became lithified. Later, the mollusk dissolved away, leaving behind a steinkern (internal cast). In thin section, moldic pores occur as voids within a lime-mud matrix or as hollow micrite envelopes. These moldic pores are in some cases filled by pore-filling calcite cement. However, even the pore-filling cements in some cases show evidence of later solution. Non-fabric-selective dissolution has created vugs, especially in well-lithified lime mud.

Post-Meteoric Shallow-Marine Diagenesis

Evidence of marine diagenesis that took place after subaerial exposure is found in last-generation highly unstable Mg calcite cements and internal sediments found in limestones that have otherwise been almost wholly stabilized to calcite. Post-meteoric marine diagenesis (Fig. 11) is most evident in zone 1 and 2 limestones. While large parts of these limestones

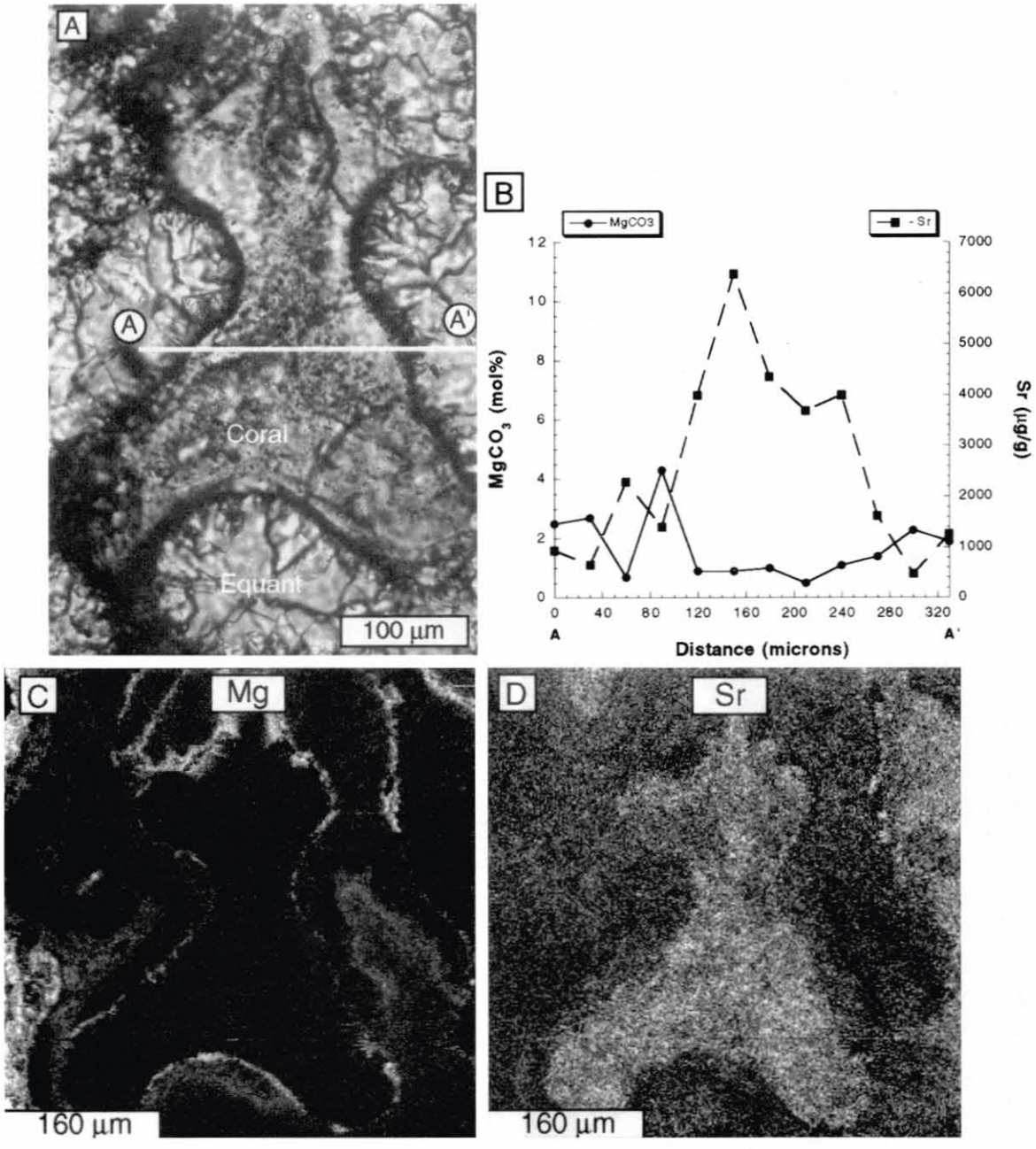

FIG. 8.—Neomorphism of coral skeleton. **A)** Fabric-selective mosaic. Coral skeleton composed of coarse mosaic of neomorphic calcite spar, center. Crystals of this mosaic do not extend beyond the skeleton. Residual organic matter imparts a darkened appearance to the former coral skeleton, while surrounding, finer, void-filling equant calcite cement is generally clear. Dark coating on coral may be early marine microcrystalline cement. Thin section, plane-polarized light. **B)** Microprobe traverse of $MgCO_3$ (filled circles) and Sr (filled squares) across void-filling cement and neomorphic spar (A to A'). $MgCO_3$ is relatively constant between void-filling cement and neomorphic spar. However, the neomorphic spar is enriched in Sr compared to the void filling, which is consistent with its originally aragonite mineralogy. **C)** Microprobe map of Mg. Density of white spots reflects abundance of Mg. Mg is relatively constant throughout. There is a slight enrichment bordering the coral skeleton that corresponds to dark coating in A and may be a remnant of an early marine Mg calcite cement. **D)** Microprobe map of Sr. Density of white spots reflects abundance of Sr. Neomorphic spar is enriched with Sr relative to surrounding void-filling cement.

have been stabilized to calcite, solutional voids are commonly lined by thick (up to 300 μm) isopachous rims of bladed Mg calcite spar and/or contain Mg calcite-rich internal sediment. These thick bladed rims are commonly composed of a series of partial spherulites or splays nucleated at points along the substrate (cf. James and Ginsburg 1979). This microstructure creates a mammilated surface (millimeter-size mammelons) visible in hand sample (see Fig. 11). Isopachous rims of bladed Mg calcite also occur on calcitized coral skeletons in which original skeletal microstructure has been entirely replaced by a mosaic of neomorphic calcite spar. The Mg calcite cements and internal sediments appear to be in pristine condition, i.e., they have retained uniform high-magnesium contents and show no evidence of solution or meteoric alteration. In contrast, first-generation early marine cements have highly variable magnesium contents.

Numerous studies (see Bischoff et al. 1993; Morse and Mackenzie 1990; and references therein) have demonstrated that, in general, the first diagenetic event to take place in the meteoric regime is the loss of magnesium from highly chemically reactive Mg calcites (those with $>$ 12 mole % $MgCO_3$). This event is then followed by the gradual disappearance of aragonite and replacement by calcite. It has been demonstrated that both of these meteoric diagenetic events have taken place in the zones 1 and 2 limestones. The last-generation Mg calcite cements contain an average of $\sim$ 15 mole % $MgCO_3$. Experimental data indicate that magnesian calcite

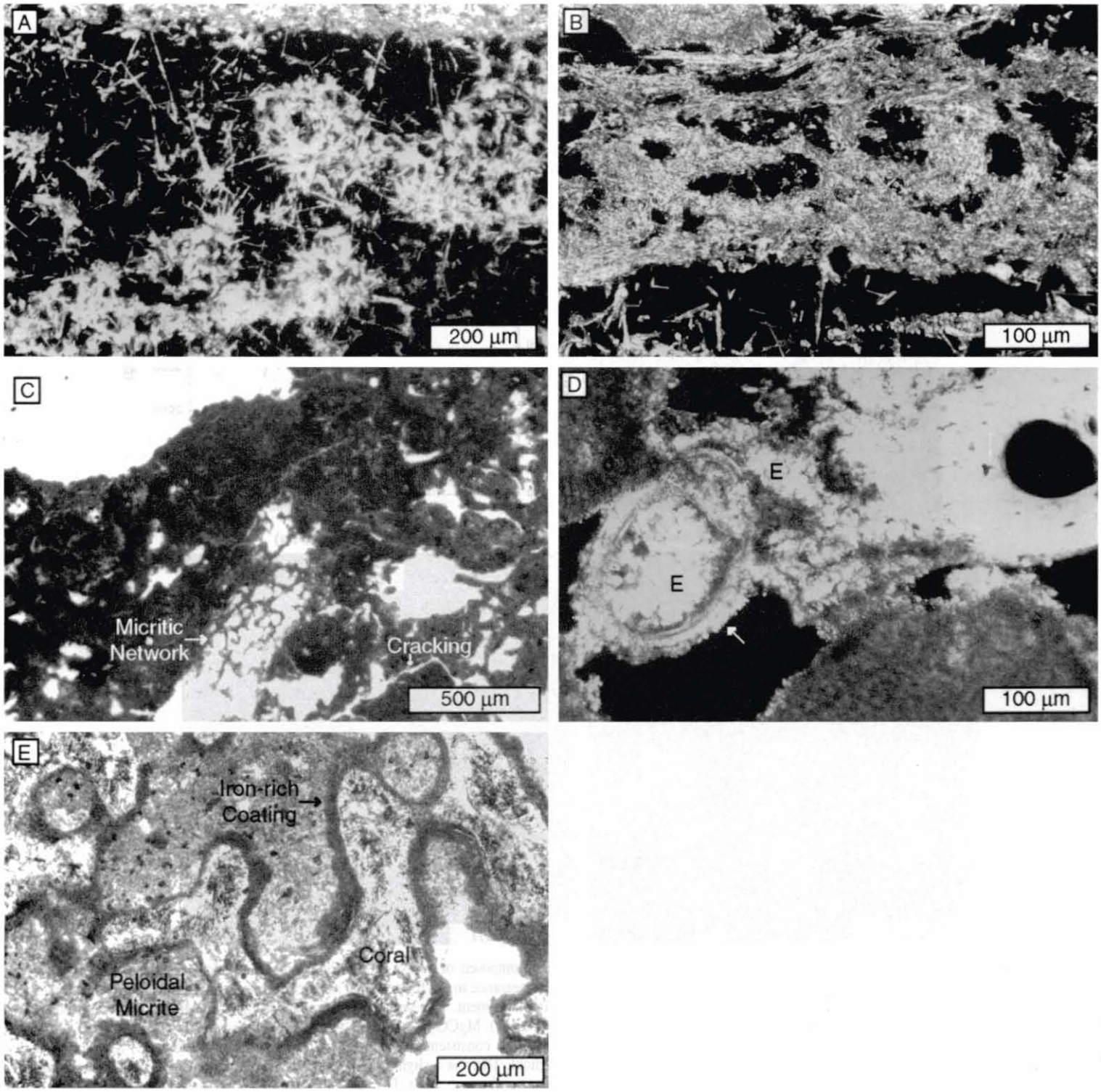

FIG. 9.—Products of subaerial exposure and meteoric diagenesis. **A)** Random calcite needle fibers forming loosely woven network in void. Thin section, crossed polars. **B)** Tangential calcite needle fibers forming interconnected bridge-like bands across voids. Thin section, crossed polars. **C)** Clotted micrite from Pleistocene subaerial exposure surface. Clotted texture formed by irregular clumps of micrite separated by large irregular voids, channels, and cracks. Anastomosing micritic network (alveolar texture) occupies large void in center of photomicrograph. Thin section, plane-polarized light. **D)** Equant calcite (E) forming drusy, void-filling cement within miliolid foraminifer (arrow), left center, and replacing micritic cement at grain contacts, center. Thin section, crossed polars. **E)** Discolored coral with coating of iron-rich noncarbonate clay. Light-colored peloidal Mg calcite occupying voids is a post-meteoric cement. Thin section, plane-polarized light.

with $>$ 12 mole % $MgCO_3$ is less stable than aragonite as well as calcites with lower magnesium contents (Walter 1985). Thus, it is reasonable to conclude that last-generation Mg calcite cements (those with $>$ 12 mole % $MgCO_3$) were formed after stabilization of the surrounding limestone to calcite. It is possible that all Mg calcite cements were formed prior to subaerial exposure and that some of these were simply not altered in the meteoric environment. The solubility of Mg calcite is controlled not only by magnesium content but also by other chemical and physical properties of the solid (Bischoff et al. 1993). However, there is abundant evidence of alteration (Mg^{2+} loss) of first-generation Mg calcite cements (Fig. 7) as well as Mg calcite skeletal grains (Fig. 11). It is only the last-generation pore-lining cements that have retained a uniform Mg calcite composition. It is also possible that the cements were stabilized without a loss of magnesium. However, evidence of this is very rare in the rock record (Bischoff

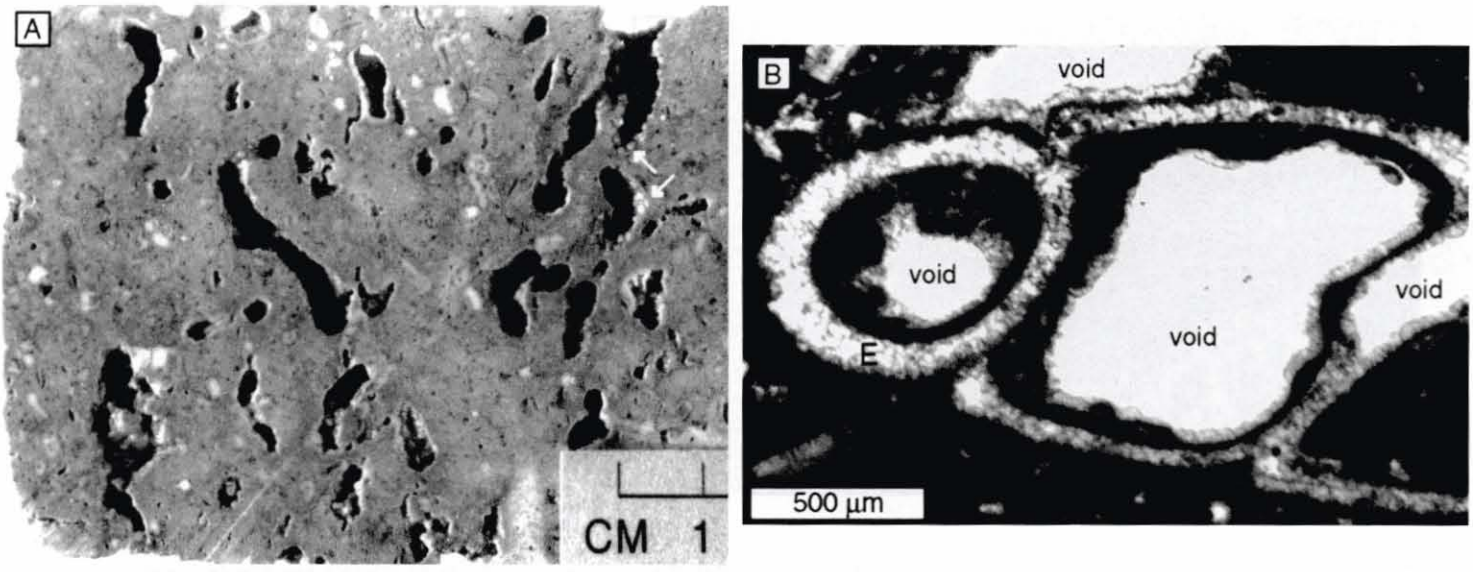

FIG. 10.—Dissolution features. **A)** Macroscopic view of moldic porosity in branching-coral facies. Voids caused by dissolution of aragonitic, delicate branching coral (*Pocillopora damicornis*). Voids retain impression of the external surface of the coral (external mold) (arrows). **B)** Moldic pore left behind after dissolution of gastropod. Mold is partially filled by equant calcite spar (E). Thin section, plane-polarized light.

et al. 1993). Therefore, last-generation Mg calcite cements and internal sediments that occur directly on limestone substrates that have otherwise been almost wholly stabilized to calcite provide evidence of marine diagenesis following subaerial exposure and meteoric diagenesis. It is unlikely that all of the Mg calcite and aragonite in the surrounding rock would have stabilized to calcite while leaving just last-generation, pore-lining, highly chemically reactive Mg calcite cements (both sparry and microcrystalline) unaffected. The pristine condition of these cements suggests that they have not been exposed to a meteoric environment. Thus, they most probably represent recent marine diagenesis that has occurred following the resubmergence of the nearshore terrace during the last deglaciation.

DISCUSSION

Although Quaternary carbonates form an important component of the subaerial and nearshore geology of Oahu, relatively little is known about the timing and nature of formation of much of this record. Deep cores taken on the Ewa Plain (Stearns and Chamberlain 1967) contain a record of at least eight transgressive/regressive cycles (Resig 1969). These cycles, however, have never been fully correlated with the marine oxygen isotope record. Emerged limestones such as the Waimanalo Formation, which reaches elevations as high as +12.5 m, have been correlated with marine oxygen isotope substage 5e (Ku et al. 1974; Szabo et al. 1994). The Kaena Formation, reaching +30 m, has been correlated with marine oxygen isotope stages 13 or 15 (Szabo et al. 1994). A record of Holocene reef growth in Hanauma Bay was described by Easton and Olson (1976). Emerged Holocene marine deposits have been described by Fletcher and Jones (1996). This represents our state of knowledge of Quaternary carbonate deposition on Oahu. Thus, a large part of the Quaternary has not been clearly identified in the stratigraphy of Oahu, namely the periods between deposition of the Kaena and Waimanalo Formations (~ 500 ka to ~ 125 ka, including marine oxygen isotope stages 11, 9, and 7), and the Waimanalo Formation and Holocene deposits (~ 125 ka to ~ 7 ka, including marine oxygen isotope stages 5c, 5a, and 3) (Fig. 12). Cores taken at Waimanalo (Lum and Stearns 1970) indicate that a thick, subaerial eolianite separates the Kaena and Waimanalo Formations. At Barbers Point an unconformity spanning perhaps 400 thousand years separates these units (Sherman et al. 1993) (Table 2). The limited number of Th–U ages presented here of fossil corals from the nearshore terrace of Oahu indicates that much of the "missing record" may be found in the nearshore submarine terraces of Oahu.

The shoreward zonation of facies is consistent with the expected zonation of facies in a marginal reef complex (cf. Longman 1981; James and Bourque 1992), suggesting that the massive-coral facies acted as a barrier creating a protected, back-reef setting where the branching-coral facies was deposited. Thus, the nearshore terrace of Oahu represents an *in situ* fossil mature reef complex.

Th–U ages of fossil corals and the similarity of diagenetic history (i.e., suggesting a similarity in age) among adjacent limestones suggest that the fossil reef complex was formed during marine oxygen isotope stage 7. However, lower parts of the seaward front of the terrace, zone 3, yield Th–U ages that correlate with marine oxygen isotope substages 5a and 5c. The broad range of ages found indicate the complexity of the internal structure of the terrace, reflecting stages of accretion during several interglacial highstands. We suggest that most of the terrace is composed of an *in situ* stage 7 reef complex. Later, substage 5c and substage 5a accretion occurred along the deep seaward margin of the terrace, while the upper parts of the terrace remained subaerial (Fig. 13). Additional coring and radiometric age dating, currently underway, will help to better determine the internal stratigraphy and timing of terrace formation.

Extensive early marine cementation in the zone 2 (stage 7) massive-coral facies is consistent with its formation in a high-energy environment. Marine cementation is favored and, thus, most pervasive, near the sediment–water interface in high-energy environments, where water can be flushed through the porous structure of the reef (Macintyre 1977). Tucker and Wright (1990) refer to this as the active marine phreatic zone. The lack of early marine cementation and dominance of micritization in the branching-coral facies is consistent with its deposition in a low-energy back-reef environment. The lack of early marine cementation may be explained by lower rates of seawater being flushed through the sediments, because of its deposition in a relatively low-energy environment, and the lower permeability of the lime-mud matrix. Tucker and Wright (1990) referred to this environment as the stagnant marine phreatic zone, where there is little sediment or pore-fluid movement, microbial micritization of grains is ubiquitous, and cementation is limited. The absence of cementation in protected back-reef areas of fringing and barrier reefs is common in modern reef environments (James et al. 1976; Macintyre 1977; Lighty 1985).

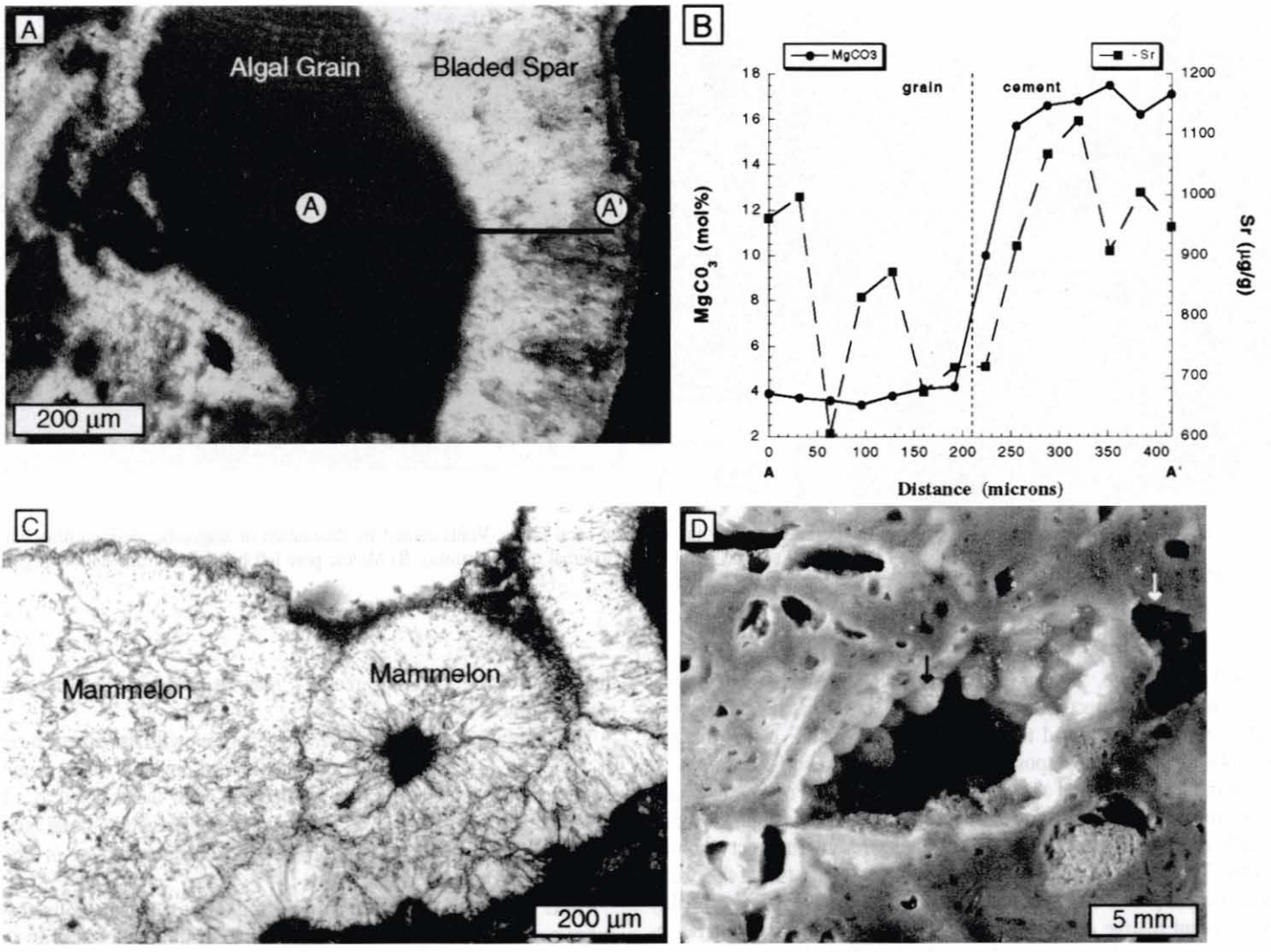

FIG. 11.—Post-meteoric marine cement. **A)** Altered algal grain with isopachous rim of bladed spar. Thin section, crossed polars. **B)** Microprobe traverse of $MgCO_3$ (filled circles) and Sr (filled squares) across algal grain and isopachous rim of bladed spar (A to A'). Coralline algae is originally composed of Mg calcite. However, microprobe analyses show that this grain has lost Mg^{2+} to solution in a meteoric environment and is now composed of calcite (avg. content, 3.8 mole % $MgCO_3$). In contrast, the isopachous rim of bladed spar is composed of Mg calcite (avg. content, 15.7 mole % $MgCO_3$). Sr is more variable but has a somewhat lower average concentration (808 μg/g) in the algal grain than in the cement (955 μg/g). These data suggest that following deposition this unit was emerged above sea level and underwent meteoric diagenesis (e.g., leaching of Mg^{2+}). This was followed by submergence and precipitation of post-meteoric marine cements. **C)** Mammelons of bladed Mg calcite spar partially filling solution void. Thin section, plane-polarized light. **D)** Macroscopic view of bladed Mg calcite mammelons (black arrow) lining solutional void in coral floatstone. Surrounding limestone is almost wholly stabilized to calcite. Aragonitic corals have largely dissolved, leaving behind moldic pores (white arrow). Only last-generation pore-lining cements are composed of unstable Mg calcite

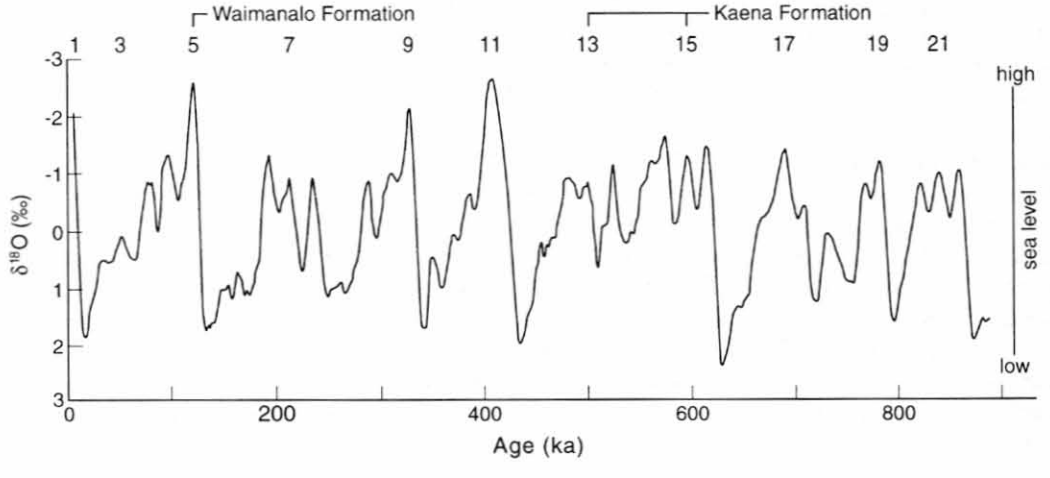

FIG. 12.—Low-latitude Late Pleistocene $\delta^{18}O$ reference record (Bassinot et al. 1994) and correlations of the Waimanalo and Kaena Formations with interglacial periods, indicated by odd-numbered marine isotope stages (after Muhs and Szabo 1994; Szabo et al. 1994).

TABLE 2.—*Pleistocene stratigraphy at two coastal sites on Oahu correlated to marine oxygen isotope record.*

Barbers Point[1]			Waimanalo[2]		
Stratigraphic Unit	Lithology	Isotope Stage[1,3]	Stratigraphic Unit	Lithology	Isotope Stage[1,3]
				Carbonate Sand	
			Unnamed		1
V-Waimanalo Fm	Bafflestone	5e	–unconformity–	Reef Limestone	
IV-Waimanalo Fm	Beachrock		Waimanalo Fm		5e
III-Waimanalo Fm	Rudstone		–unconformity–	Eolianite	
II-Waimanalo Fm	Bafflestone	5c	Bellows Field Fm		?
–unconformity–			–unconformity–	Beachrock	
I-Kaena Fm	Boundstone	13 or 15	Kaena Fm	Reef Limestone	13 or 15
			–unconformity–		
			Kahuku Pt Fm	Beachrock	
				Reef Limestone	?
				Calcareous Clay	
			–unconformity–		
			Unnamed	Terriginous Conglomerate	?
			Unnamed	Calcareous Clay	?

[1] After Sherman et al. (1993).
[2] After Lum and Stearns (1970).
[3] Based on correlations made in Szabo et al. (1994).

During periods of emergence meteoric alteration of limestones occurred in the meteoric vadose zone. There is no conclusive evidence that these limestones were exposed to a meteoric phreatic environment. Although the zones 1 and 2, stage 7, limestones likely underwent two complete cycles of emergence and submergence (Fig. 13), multiple generations of meteoric cements were not observed. Thus, the diagenetic record in these limestones appears to be incomplete.

Post-meteoric marine cementation in the branching-coral facies is more extensive than early marine cementation. This implies a change in diagenetic environment from stagnant marine phreatic, during deposition of the branching-coral facies, to the present active marine phreatic environment favoring marine cementation. During periods of emergence, the branching-coral facies was lithified and stabilized to calcite in a meteoric environment and underwent partial solution and creation of vug and channel porosity. Upon submergence into the marine environment, it appears that the stable, lithified substrate along with conduit or channel-type porosity has led to high flow rates induced by channelized seawater. This, in turn, resulted in precipitation of thick (up to 300 μm), isopachous rims of bladed Mg calcite spar lining the walls of large voids (cf. McCullough and Land 1992). In some instances, voids are lined or partially filled by a combination of micritic crusts and internal sediments. Their association with cavities again suggests that enhanced flow probably occurred and was an important aspect of their formation. During coring operations, the authors noted that wave energy was capable of moving large volumes of water through the fossil reef substrate.

The general trend of decreasing mineralogic stabilization (decreasing calcite content) from zones 1 through 3 is consistent with the Th–U ages of fossil corals from these deposits, i.e., less mineralogic stabilization in the younger limestones. However, the bulk mineralogy of some samples can be deceiving, because post-meteoric marine cementation may produce a mineralogically "rejuvenated" limestone. This appears to be the case in the zone 1 limestones, where much of the Mg calcite detected in XRD analyses probably reflects last-generation, post-meteoric, shallow-marine cements and internal sediments. Most of the components of these limestones, including mixed skeletal grains and lime mud matrix, are composed of calcite. Therefore, it is important to examine the mineralogic composition of the original skeletal components as well as cement generations to determine the diagenetic history of a limestone.

One interesting outcome of this research lies in what was not found. In 24 separate cores covering ~ 10 km of coastline and ranging between water depths of ~ 5.5 and 35 m, no evidence of Holocene accretion was found. Rather, the seafloor is undergoing extensive biological and physical erosion. Signatures of subaerial exposure and meteoric diagenesis are recognized in the upper several centimeters of all cores. Thus, the present seafloor in the study area represents a flooded Pleistocene subaerial exposure surface. Holocene accretion is limited to sparse patches of coral and coralline-algal growth. Holocene reef accretion in Hawaii appears to be largely limited by wave forces (Dollar 1982; Grigg 1983; Dollar and Tribble 1993). Episodic destruction of coral communities by storms and open-ocean swell and the removal of carbonate material from nearshore reef zones prevents cementation, lithification, and reef accretion (Dollar and Tribble 1993). Why extensive and thick reef sequences along this coast were able to develop during the Pleistocene but not during the Holocene remains a question for future research.

CONCLUSIONS

(1) All limestones found in cores from a nearshore terrace on Oahu are typical of shallow-marine, reef environments and comprise either a branching-coral or massive-coral facies. The shoreward zonation of facies

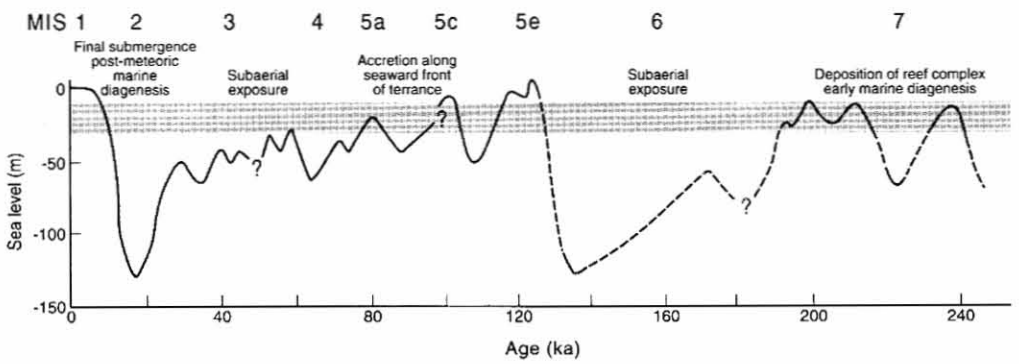

FIG. 13.—Relationship between late Pleistocene sea-level fluctuations, terrace formation/reef accretion, and stages of marine and meteoric diagenesis. Gray band indicates the position of the nearshore terrace. Sea-level curve from Chappell and Shackleton (1986). MIS = Marine isotope stage.

suggests that the nearshore terrace represents an *in situ*, fossil mature reef complex.

(2) Th–U ages of *in situ* corals indicate that the nearshore terrace is Pleistocene in age. Most of the terrace is composed of a fossil reef complex formed during marine oxygen isotope stage 7. Later accretion along the seaward front of the terrace occurred during marine oxygen isotope substages 5a and/or 5c. No Holocene limestones were recovered. The present seafloor in the study area represents a Pleistocene subaerial exposure surface.

(3) There is a general trend of increasing mineralogic stabilization of limestones, as determined by XRD, with increasing absolute age as determined by Th–U techniques. The present mineralogic composition of the limestones is a reflection of their original skeletal composition and early marine cementation, meteoric alteration and cementation, and post-meteoric marine cementation that followed their submergence during the last deglaciation.

(4) Early marine diagenesis is most prevalent in the marginal high-energy massive-coral facies. The low-energy branching-coral facies displays little evidence of early marine cementation. Post-meteoric marine cementation is evident in all lithofacies and reflects recent processes operating since the last deglaciation in an active marine phreatic environment.

ACKNOWLEDGMENTS

This research was supported by the National Science Foundation (EAR-9710005), the U.S. Geological Survey, and the National Geographic Society. John Rooney provided extensive and exhaustive assistance in the field. Cliff Todd assisted with the microprobe analyses. The authors would also like to thank I. Macintyre, M. Coniglio, and Associate Editor B. Jones for their critical reviews and helpful suggestions that improved the manuscript. The final editing of Corresponding Editor J. Southard improved the clarity and smoothness of reading. School of Ocean and Earth Science and Technology contribution No. 4782.

REFERENCES

Bain, R.J., and Foos A.M., 1993, Carbonate microfabrics related to subaerial exposure and paleosol formation, *in* Rezak, R., and Lavoie, D.L., eds., Carbonate Microfabrics: New York, Springer-Verlag, p. 19–27.

Bard, E., Hamelin, B., Arnold, M., Montaggioni, L., Cabioch, G., Faure, G., and Rougerie, F., 1996a, Deglacial sea-level record from Tahiti corals and the timing of global meltwater discharge: Nature, v. 382, p. 241–244.

Bard, E., Jouannic, C., Hamelin, B., Pirazzoli, P., Arnold, M., Faure, G., Sumosusastro, P., and Syaefudin, 1996b, Pleistocene sea levels and tectonic uplift based on dating of corals from Sumba Island, Indonesia: Geophysical Research Letters, v. 23, p. 1473–1476.

Bassinot, F.C., Labeyrie, L.D., Vincent, E., Quidelleur, X., Shackleton, N.J., and Lancelot, Y., 1994, The astronomical theory of climate and the age of the Brunhes–Matuyama magnetic reversal: Earth and Planetary Science Letters, v. 126, p. 91–108.

Bischoff, W.D., Bertram, M.A., Mackenzie, F.T., and Bishop, F.C., 1993, Diagenetic stabilization pathways of magnesian calcites: Carbonates and Evaporites, v. 8, p. 82–89.

Bischoff, W.D., Bishop, F.C., and Mackenzie, F.T., 1983, Biogenically produced magnesian calcite: Inhomogeneities in chemical and physical properties; comparison with synthetic phases: American Mineralogist, v. 68, p. 1183–1188.

Bosence, D., 1985, Preservation of coralline-algal reef frameworks: Fifth International Coral Reef Congress, Tahiti, Proceedings, v. 6, p. 623–628.

Budd, D.A., and Hiatt, E.E., 1993, Mineralogical stabilization of high-magnesium calcite: geochemical evidence for intracrystal recrystallization within porcellaneous Foraminifera: Journal of Sedimentary Petrology, v. 63, p. 261–274.

Chappell, J., and Shackleton, N.J., 1986, Oxygen isotopes and sea level: Nature, v. 324, p. 137–140.

Chen, J.H., Edwards, R.L., and Wasserburg, G.J., 1986, ^{238}U, ^{234}U and ^{232}Th in seawater: Earth and Planetary Science Letters, v. 80, p. 241–251.

Choquette, P.W., and Trusell, F.C., 1978, A procedure for making the titan-yellow stain for Mg-calcite permanent: Journal of Sedimentary Petrology, v. 48, p. 639–641.

Coulbourn, W.T., Campbell, J.F., and Moberly, R., 1974, Hawaiian submarine terraces, canyons, and Quaternary history evaluated by seismic-reflection profiling: Marine Geology, v. 17, p. 215–234.

de Bievre, P., Lauer, K.F., le Duigou, Y., Moret, H., Muschenborn, G., Spaepen, J., Spernol, A., Vaninbroukx, R., and Verdingh, V., 1971, The half-life of ^{234}U, *in* Hurrell, M.L., ed., Chemical Nuclear Data—Measurement and Applications: Proceedings of the International Conference Organized by the British Nuclear Energy Society: London, Institution of Civil Engineers, p. 221–225.

Dollar, S.J., 1982, Wave stress and coral community structure in Hawaii: Coral Reefs, v. 1, p. 71–81.

Dollar, S.J., and Tribble, G.W., 1993, Recurrent storm disturbance and recovery: a long-term study of coral communities in Hawaii: Coral Reefs, v. 12, p. 223–233.

Dunham, R.J., 1962, Classification of carbonate rocks according to depositional texture, *in* Ham, W.E., ed., Classification of Carbonate Rocks: American Association of Petroleum Geologists, Memoir 1, p. 108–121.

Dunham, R.J., 1971, Meniscus cement, *in* Bricker, O.P., ed., Carbonate Cements: Johns Hopkins University, Studies in Geology, no. 19, p. 297–300.

Easton, W.H., and Olson, E.A., 1976, Radiocarbon profile of Hanauma reef, Oahu, Hawaii: Geological Society of America, Bulletin, v. 87, p. 711–719.

Edwards, R.L., Chen, J.H., and Wasserburg, G.J., 1986/87, ^{238}U–^{234}U–^{230}Th–^{232}Th systematics and the precise measurement of time over the past 500,000 years: Earth and Planetary Science Letters, v. 81, p. 175–192.

Embry, A.F., and Klovan, J.E., 1971, A Late Devonian reef tract on north-eastern Banks Island, N.W.T.: Bulletin of Canadian Petroleum Geology, v. 19, p. 730–781.

Esteban, M., and Klappa, C.F., 1983, Subaerial exposure environment, *in* Scholle, P.A., Bebout, D.G., and Moore, C.H., eds., Carbonate Depositional Environments: American Association of Petroleum Geologists, Memoir 33, p. 1–95.

Fletcher, C.H., and Jones, A.T., 1996, Sea-level highstand recorded in Holocene shoreline deposits on Oahu, Hawaii: Journal of Sedimentary Research, v. 66, p. 632–641.

Fletcher, C.H., and Sherman, C.E., 1995, Submerged shorelines on O'ahu, Hawai'i: Archive of episodic transgression during the deglaciation?, *in* Finkl, C.W., ed., Holocene Cycles: Climate, Sea Levels and Sedimentation: Journal of Coastal Research, Special Issue 17, p. 141–152.

Gallup, C.D., Edwards, R.L., and Johnson, R.G., 1994, The timing of high sea levels over the past 200,000 years: Science, v. 263, p. 796–800.

Ginsburg, R.N., Marszalek, D.S., and Schneidermann, N., 1971, Ultrastructure of carbonate cements in a Holocene algal reef of Bermuda: Journal of Sedimentary Petrology, v. 41, p. 472–482.

Grigg, R.W., 1983, Community structure, succession and development of coral reefs in Hawaii: Marine Ecology Progress Series, v. 11, p. 1–14.

Grossman, E.E., and Fletcher, C.H., 1998, Sea level higher than present 3500 years ago on the northern main Hawaiian Islands: Geology, v. 26, p. 363–366.

Jaffey, A.H., Flynn, K.F., Glendenin, L.E., Bentley, W.C., and Essling, A.M., 1971, Precision measurement of half-lives and specific activities of ^{235}U and ^{238}U: Physical Review C, v. 4, p. 1889–1906.

James, N.P., 1972, Holocene and Pleistocene calcareous crust (caliche) profiles: criteria for subaerial exposure: Journal of Sedimentary Petrology, v. 42, p. 817–836.

James, N.P., 1983, Reef environment, *in* Scholle, P.A., Bebout, D.G., and Moore, C.H., eds., Carbonate Depositional Environments: American Association of Petroleum Geologists, Memoir 33, p. 345–462.

James, N.P., and Bourque, P.-A., 1992, Reefs and mounds, *in* Walker, R.G., and James, N.P., eds., Facies Models: Response to Sea Level Change: Geological Association of Canada, p. 323–347.

James, N.P., and Ginsburg, R.N., 1979, The Seaward Margin of Belize Barrier and Atoll Reefs: International Association of Sedimentologists, Special Publication 3, 191 p.

James, N.P., Ginsburg, R.N., Marszalek, D.S., and Choquette, P.W., 1976, Facies and fabric specificity of early subsea cements in shallow Belize (British Honduras) reefs: Journal of Sedimentary Petrology, v. 46, p. 523–544.

Jones, A.T., 1993, Elevated fossil coral deposits in the Hawaiian Islands: A measure of island uplift in the Quaternary [unpublished Ph.D. thesis]: University of Hawaii, Honolulu, 274 p.

Jones, A.T., 1994, Review of the chronology of marine terraces in the Hawaiian Archipelago: Quaternary Science Reviews, v. 12, p. 811–823.

Ku, T.L., Kimmel, M.A., Easton, W.H., and O'Neil, T.J., 1974, Eustatic sea level 120,000 years ago on Oahu, Hawaii: Science, v. 183, p. 959–962.

Lighty, R.G., 1985, Preservation of internal reef porosity and diagenetic sealing of submerged early Holocene barrier reef, southeast Florida Shelf, *in* Schneidermann, N., and Harris, P.M., eds., Carbonate Cements: SEPM, Special Publication 36, p. 123–151.

Longman, M.W., 1980, Carbonate diagenetic textures from nearshore diagenetic environments: American Association of Petroleum Geologists, Bulletin, v. 46, p. 461–487.

Longman, M.W., 1981, A process approach to recognizing facies of reef complexes, *in* Toomey, D.F., ed., European Fossil Reef Models: SEPM, Special Publication 30, p. 9–40.

Lounsbury, M., and Durham, R.W., 1971, The alpha half-life of ^{234}U, *in* Hurrell, M.L., ed., Chemical Nuclear Data—Measurement and Applications: Proceedings of the International Conference Organized by the British Nuclear Energy Society: London, Institution of Civil Engineers, p. 215–219.

Lum, D., and Stearns, H.T., 1970, Pleistocene stratigraphy and eustatic history based on cores at Waimanalo, Oahu, Hawaii: Geological Society of America, Bulletin, v. 81, p. 1–16.

Macintyre, I.G., 1977, Distribution of submarine cements in a modern fringing reef, Galeta Point, Panama: Journal of Sedimentary Petrology, v. 47, p. 503–516.

Macintyre, I.G., 1984, Extensive submarine lithification in a cave in the Belize barrier reef platform: Journal of Sedimentary Petrology, v. 54, p. 221–235.

Macintyre, I.G., 1985, Submarine cements—the peloidal question, *in* Schneidermann, N., and Harris, P.M., eds., Carbonate Cements: SEPM, Special Publication 36, p. 109–116.

Macintyre, I.G., and Marshall, J.F., 1988, Submarine lithification in coral reefs: Some facts and misconceptions: Sixth International Coral Reef Congress, Australia, Proceedings, v. 1, p. 263–272.

Macintyre, I.G., and Reid, R.P., 1995, Crystal alteration in a living calcareous alga (*Halimeda*): Implications for studies in skeletal diagenesis: Journal of Sedimentary Research, v. A65, p. 143–153.

Macintyre, I.G., and Reid, R.P., 1998, Recrystallization in living porcelaneous foraminifera (*Archaias angulatis*): Textural changes without mineral alteration: Journal of Sedimentary Research, v. 68, p. 11–19.

Maragos, J.E., 1977, Order Scleractinia, stony corals, *in* Devaney, D.M., and Eldredge, L.G., eds., Reef and Shore Fauna of Hawaii, Section 1: Protozoa through Ctenophora: Bernice P. Bishop Museum, Special Publication 64 (1), p. 158–241.

Marshall, J.F., 1983, Submarine cementation in a high-energy platform reef: One Tree Reef, southern Great Barrier Reef: Journal of Sedimentary Petrology, v. 53, p. 1133–1149.

McCullough, M.L., and Land, L.S., 1992, Dynamic hydrology and diagenesis of a submerged Pleistocene fringing reef, Discovery Bay, Jamaica: Marine Geology, v. 104, p. 139–151.

McKee, E.D., and Ward, W.C., 1983, Eolian environment, *in* Scholle, P.A., Bebout, D.G., and Moore, C.H., eds., Carbonate Depositional Environments: American Association of Petroleum Geologists, Memoir 33, p. 131–170.

Meadows, J.W., Armani, R.J., Callis, E.L., and Essling, A.M., 1980, Half-life of ^{230}Th: Physical Review C, v. 22, p. 750–754.

Meyers, J.H., 1987, Marine vadose beachrock cementation by cryptocrystalline magnesian calcite—Maui, Hawaii: Journal of Sedimentary Petrology, v. 57, p. 558–570.

Moore, J.G., 1987, Volcanism in Hawaii. Subsidence of the Hawaiian Ridge: U.S. Geological Survey, Professional Paper 1350, p. 85–100.

Morse, J.W., and Mackenzie, F.T., 1990, Geochemistry of Sedimentary Carbonates: New York, Elsevier, Developments in Sedimentology 48, 707 p.

Muhs, D.R., and Szabo, B.J., 1994, New uranium-series ages of the Waimanalo Limestone, Oahu, Hawaii: Implications for sea level during the last interglacial period: Marine Geology, v. 118, p. 315–326.

Pierson, B.J., and Shinn, E.A., 1985, Cement distribution and carbonate mineral stabilization in Pleistocene limestones of Hogsty Reef, Bahamas, *in* Schneidermann, N., and Harris, P.M., eds., Carbonate Cements: SEPM, Special Publication 36, p. 153–168.

Pingitore, N.E., Jr., 1976, Vadose and phreatic diagenesis: Processes, products, and their recognition in corals: Journal of Sedimentary Petrology, v. 46, p. 985–1006.

Reid, R.P., Macintyre, I.G., and Post, J.E., 1992, Micritized skeletal grains in northern Belize lagoon: A major source of Mg-calcite mud: Journal of Sedimentary Petrology, v. 62, p. 145–156.

Resig, J., 1969, Paleontological investigations of deep borings on the Ewa Plain, Oahu, Hawaii: Hawaii Institute of Geophysics, Report HIG-69–2, 99 p.

Rezak, R., and Lavoie, D.L., 1993, Recommendations, *in* Rezak, R., and Lavoie, D.L., eds., Carbonate Microfabrics: New York, Springer-Verlag, p. 303–307.

Sabine, C.L., 1992, Geochemistry of particulate and dissolved inorganic carbon in the central North Pacific [unpublished Ph.D. thesis]: University of Hawaii, Honolulu, 249 p.

Sandberg, P., 1985, Aragonite cements and their occurrence in ancient limestone, *in* Schneidermann, N., and Harris, P.M., eds., Carbonate Cements: SEPM, Special Publication 36, p. 33–57.

Scoffin, T.P., 1987, An Introduction to Carbonate Sediments and Rocks: New York, Chapman & Hall, 274 p.

Scoffin, T.P., 1993, Microfabrics of carbonate muds in reefs, *in* Rezak, R., and Lavoie, D.L., eds., Carbonate Microfabrics: New York, Springer-Verlag, p. 65–74.

Shackleton, N.J., 1987, Oxygen isotopes, ice volume and sea level: Quaternary Science Reviews, v. 6, p. 183–190.

Sherman, C.E., Glenn, C.R., Jones, A.T., Burnett, W.C., and Schwarcz, H.P., 1993, New evidence for two highstands of the sea during the last interglacial, oxygen isotope substage 5e: Geology, v. 21, p. 1079–1082.

Stearns, H.T., 1946, Geology of the Hawaiian Islands: Hawaii Division of Hydrography, Bulletin 8, 105 p.

Stearns, H.T., 1974, Submerged shorelines and shelves in the Hawaiian Islands and a revision of some of the eustatic emerged shorelines: Geological Society of America, Bulletin, v. 85, p. 795–804.

Stearns, H.T., 1978, Quaternary shorelines in the Hawaiian Islands: Bernice P. Bishop Museum, Bulletin 237, 57 p.

Stearns, H.T., and Chamberlain, T.K., 1967, Deep cores of Oahu, Hawaii and their bearing on the geologic history of the central Pacific basin: Pacific Science, v. 21, p. 153–165.

Szabo, B.J., Ludwig, K.R., Muhs, D.R., and Simmons, K.R., 1994, Thorium-230 ages of corals and duration of the last interglacial sea-level high stand on Oahu, Hawaii: Science, v. 266, p. 93–96.

Tucker, M.E., and Wright, V.P., 1990, Carbonate Sedimentology: Oxford, U.K., Blackwell Scientific Publications, 482 p.

Veeh, H.H., 1966, Th^{230}/U^{238} and U^{234}/U^{238} ages of Pleistocene high sea level stand: Journal of Geophysical Research, v. 71, p. 3379–3386.

Videtich, P.E., 1985, Electron microprobe study of Mg distribution in recent Mg calcites and recrystallized equivalents from the Pleistocene and Tertiary: Journal of Sedimentary Petrology, v. 55, p. 421–429.

Vollbrecht, R., and Meischner, D., 1996, Diagenesis in coastal carbonates related to Pleistocene sea level, Bermuda Platform: Journal of Sedimentary Research, v. 66, p. 243–258.

Walter, L.M., 1985 Relative reactivity of skeletal carbonates during dissolution: Implications for diagenesis, *in* Schneidermann, N., and Harris, P.M., eds., Carbonate Cements: SEPM, Special Publication 36, p. 3–16.

Watts, A.B., and ten Brink, U.S., 1989, Crustal structure, flexure, and subsidence history of the Hawaiian Islands: Journal of Geophysical Research, v. 94, p. 10,473–10,500.

Whittle, G.L., Kendall, C.G.St.C., Dill, R.F., and Rouch, L., 1993, Carbonate cement fabrics displayed: A traverse across the margin of the Bahamas Platform near Lee Stocking Island in the Exuma Cays: Marine Geology, v. 110, p. 213–243.

Received 18 May 1998; accepted 25 November 1998.